TECHNISCHE UNIVERSITÄT WIEN
Vienna University of Technology

DIPLOMARBEIT

Site-directed mutagenesis and purification studies of recombinant glycosylated horseradish peroxidase

Ausgeführt am Institut für Biochemical Engineering

der Technischen Universität Wien

unter der Anleitung von

Univ.Prof. Dr. Christoph Herwig

und

Univ.Ass. Dipl.-Ing. Dr.nat.techn. Oliver Spadiut

durch

Laura Rossetti

Weidmanngasse 15/46, 1170 Wien

Wien, 02.04.2014

CONTENTS

Abstract

To date, the enzyme horseradish peroxidase (HRP), which is frequently applied in industry and medicine, is mainly isolated from the horseradish root. Because of the cumbersome purification from the plant-source, many attempts to express the enzyme in different recombinant hosts have been progressed but several steps are required to obtain purified enzyme and yields are low. Yeasts, such as *Saccharomyces cerevisiae* and *Pichia pastoris* are valuable host organisms for large scale production of heterologous glycosylated proteins. However, *P. pastoris* hyperglycosylates secreted proteins which impairs a conventional chromatographic purification.

Within the first part of this thesis, a fast and efficient 2-step protocol using hydrophobic charge induction chromatography (HCIC) and a monolithic colum for the purification of rHRP was developed, operating both systems in a negative mode. The final enzyme preparation was purified more than 12-fold from the crude fermentation broth, which makes the recombinant expression of rHRP in *P. pastoris* an interesting alternative to conventional HRP production.

Moreover, the extensive glycosylation of rHRP produced in *P. pastoris* may cause severe immunogenic responses in humans when rHRP will be applied in medicine e.g. for targeted cancer treatment. For this reason, one of the *N*-glycosylation sites present in rHRP was removed in a molecular biology approach by substituting the Asparagine residue at site N57 to the three structural similar amino acids Glutamine, Serine and Arginine. The most stable and active enzyme variant was expressed in a bioreactor and characterized thoroughly and compared to the wild type enzyme from *P. pastoris*. The final enzyme variant N57S was >2-fold more active as the wild type enzyme and had a higher thermal stability, which was achieved by substituting a single amino acid only.

Kurzfassung

Meerrettich Peroxidase (HRP) ist ein weit bekanntes Enzym welches normalerweise aus der Meerrettich-Wurzel (*Armoracia rusticana*) isoliert wird und sowohl in der Industrie als auch in der Medizin häufig angewandt wird. Aufgrund der mühsamen Gewinnung aus der Pflanze wurden viele Versuche angestellt, das Enzym mittels rekombinanter Mikroorganismen herzustellen was sich aber aufgrund der intrinsischen Eigenschaften der HRP sehr schwierig gestaltet. Hefen wie zum Beispiel *Saccharomyces cerevisiae* und *Pichia pastoris* sind bedeutende Wirtsorganismen für die Herstellung heterologer glykosylierter Proteine. Allerdings hyperglykosyliert *P. pastoris* extrazelluläre Proteine, was eine herkömmliche chromatographische Reinigung erschwert.

Im ersten Teil dieser Arbeit wurde ein schnelles und effizientes 2-stufiges Reinigungsprotokoll mittels Hydrophober-Ladungs-Induktions-Chromatographie (HCIC) und einer monolithischen Säule entwickelt, wobei beides im Negativ-Modus durchgeführt wurde. Das finale Enzympräparat wurde von der rohen Fermentationsbrühe mehr als 12-fach gereingt, was die rekombinante Herstellung von HRP eine interessante Alternative zur konventionellen Pflanzenextraktion macht.

Des Weiteren kann die Glykosylierung rekombinanter HRP Abwehrreaktionen im menschlichen Körper hervorrufen, wenn sie für medizinische Zwecke wie beispielsweise Krebstherapien verwendet werden soll. Deswegen wurde eine der 9 in HRP vorkommenden *N*-Glykosylierungsstellen durch den Austausch des Asparagin-Rests an der Stelle N57 gegen die drei strukturell ähnlichen Aminosäuren Glutamin, Serin und Asparagin in einem molekularbiologischen Ansatz entfernt. Die stabilste und aktivste Enzymvariante wurde im Bioreaktor produziert und ausführlich charakterisiert und mit dem Wild-Typ Enzym aus

P. pastoris verglichen. Die finale Enzymvariante N57S war mehr als 2-mal so aktiv und zeigte eine erhöhte thermische Stabilität, was durch Austausch einer einzigen Aminosäure erreicht wurde.

1 Background

1.1 Horseradish peroxidase

1.1.1 Description of the enzyme

Horseradish peroxidase (HRP) is a classical secretory plant peroxidase belonging to Class III peroxidases within the superfamiliy of plant peroxidases, which are of fungal, bacterial or plant origin. It is a heme-containing enzyme originating from the horseradish root (*Armoracia rusticana*) where it is present in at least 15 isoforms, ranging in its isoelectric point (pI) from 3 to 9. The neutral / neutral-basic isoform HRP C is the most abundant one in the horseradish root and thus also the most studied variant. Peroxidases are known to be involved in numerous natural defense mechanisms in plants such as lignification, cross-linking of cell wall polymers or suberin formation. However, there is still a lack of knowledge about their specific physiological functions in the plant [1].

1.1.2 Structure

The three-dimensional structure (Figure 1) and hence, the detailed catalytic mechanism of the enzyme was solved by crystallography based on HRP which was recombinantly producted in *E. Coli* [2] . For this purpose, it was particularly important to express the enzyme in a non-glycosylated form, because the heterogenous glycans severly impair the crystallization process. HRP C consists of a single polypeptide chain of 308 amino acids and hence exists in a monomeric form. The molecular weight resulting from the amino acid backbone is 34 kDa. The N-terminus is blocked by a pyroglutamate residue; the C-terminus appears heterogenic, some molecules lacking the terminal Ser308 residue. There are 4 disulfide bridges and a

buried saltbridge within the HRP molecule. Moreover, the enzyme holds two kind of metal centres: a heme-group (also referred to as iron(III) protoporphyrin IX) and two calcium atoms, which are both key structural elements for the catalytic functionality of the enzyme (Figure 1). The heme-group is located as a plane between the proximal residue His170, whereby the distal side remains unoccupied in the resting state in order to be available for H_2O_2 binding during catalytic turnover. The major part of the enzyme consists of alpha-helices, but also a small region of beta-sheets has been observed [3].

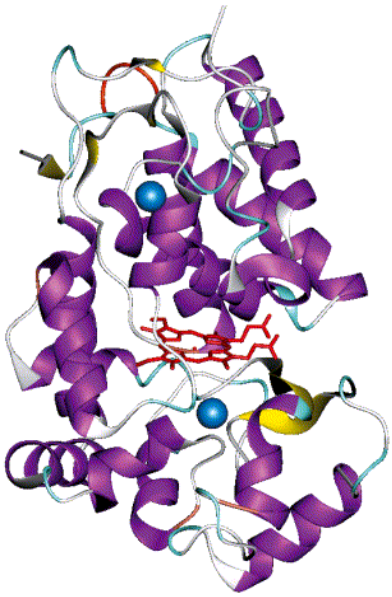

Figure 1: Three-dimensional structure of horseradish peroxidase. In the catalytic center, a heme-plane (red) and two calcium ions (blue dots) are located. The three-dimensional structure is mainly alpha-helical, but also a small region of beta-sheets is present [1].

1.1.3 Catalytic mechanism

Horseradish peroxidase is an oxidoreductase that catalyzes the reaction of a range of inorganic and organic substrates such as aromatic phenols, phenolic acids, indoles, amines, sulfonates etc as electron donors and H_2O_2 as acceptor (Equation 1) by two one-electron reduction steps through the formation of the so-called intermediates Compound I and II (Figure 2).

$$Substrate_{reduced} + H_2O_2 \longrightarrow substrate_{oxidized} + 2\ H_2O \qquad \text{(Equation 1)}$$

The catalytic conversion of a reducing substrate is initiated by the formation of Compound I which is generated by the reaction of H_2O_2 and Fe(III), whereby the Fe(IV) oxoferryl centre and a porphyrin-based cation radical is formed. Subsequently, Compound II is generated, consisting of a Fe(IV) oxoferryl species. The second part of HRP catalysis is again a one-electron reduction step, which returns Compound II back into the resting state of the enzyme, also referred to as Compound III. Compounds I and II, both are known as powerful oxidants with an electrochemical potential of + 1 V [1].

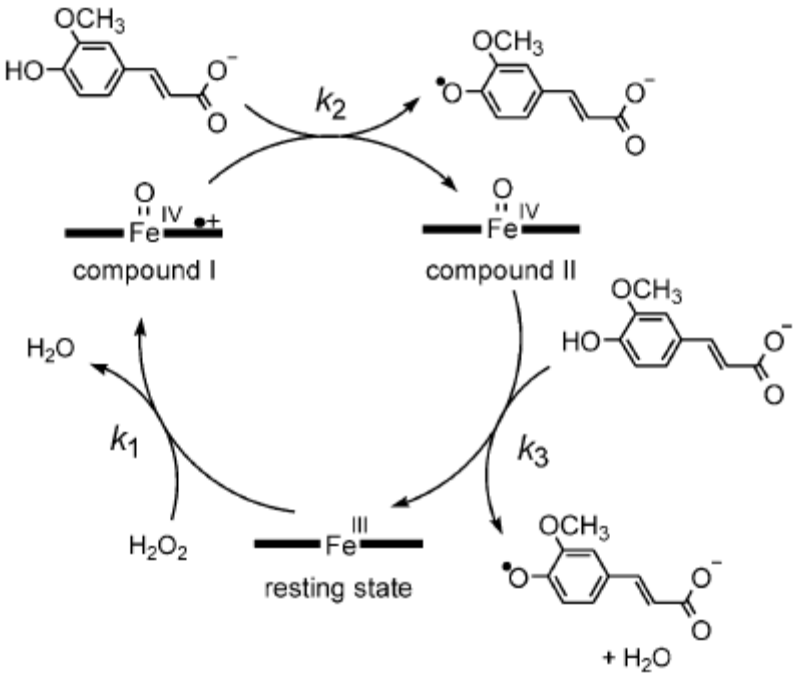

Figure 2: Catalytic cycle of HRP. The reducing substrate ferulate is converted in the two intermediate species via two one-electron reduction steps forming the two key catalytic conformations Compound I, II and the resting state, whereby k_1, k_2 and k_3 represent the respective compound formation rates [1].

1.1.4 Glycosylation

Horseradish peroxidase holds 9 potential *N*-glycosylation sites of the Asn-X-Ser/Thr type, of which 8 are occupied when the enzyme is expressed in the horseradish root. These sites are at positions N13, N57, N158, N186, N198, N214, N250, N268 which are all exposed on loop regions at the outer surface of the enzyme, thereby increasing water solubility and protecting it from radical cross-reactions [4]. Conversely, a deglycosylated enzyme showed greatly reduced solubility in salt solutions [5]. The glycan structure consists of a core structure which is composed of two N-Acetylglucosamines (GlcNAc), a Fucose (Fuc) at the innermost GlcNAc as well as a Xylose (Xyl) and three Mannose (Man) residues (Figure 3), where the carbohydrate extension is consecuted. In the plant, the *N*-glycosylation appears somehow heterogenous. Regarding the outer chains, up to 80% of the total carbohydrates present are branched heptasaccharides, but also some minor glycans have been reported. In total, 18-22% of the enzyme consists of the above described sugars, which results in an increase of the molecular weight to approximately 45 kDa [1].

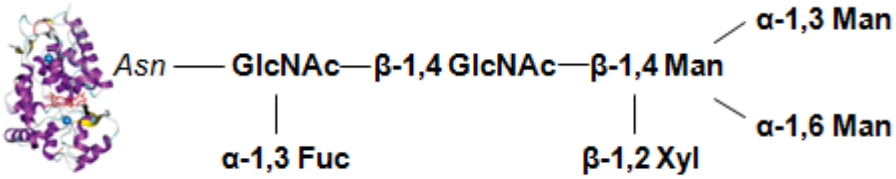

Figure 3: Glycosylation pattern of horseradish peroxidase expressed in the plant. The core structure consists of two N-Acetylglucosamines (GlcNAc), a Fucose (Fuc) at the innermost GlcNAc and a Xylose (Xyl) at the Mannose (Man) extension core.

Glycosylation has proved to be not stringently necessary for the catalytic activity of the enzyme, as the expression in *E. coli* in a non-glycosylated form yielded a fully active enzyme after refolding [2]. Moreover, when all carbohydrates except GlcNAc were removed by mild chemical deglycosylation using anhydrous trifluoromethanesulfonic acid (TFMS), the

deglycosylated homogenous enzyme showed only sixty percent activity relative to the glycosylated variant. TFMS treatment altered the physico-chemical properties by introducing negative charges to the protein and thereby allowing a simple purification using Benzhydroxamic acid affinity and ion-exchange chromatography. However, after this extensive deglycosylation procedure, only 6 percent of initial glycosylated HRP were recovered in a non-glycosylated form [5].

1.1.5 Genetic manipulations of HRP

Molecular biology techniques were used to alter the amino acid sequence and hence, to determine key catalytic amino acid residues. For example, a mutation of Phe41→Val introduced a change in substrate specificity and altered reactivity towards H_2O_2 [6]. Another study investigated mutations in the helix G region of horseradish peroxidase, which resulted in increased stabilities against heat and solvents of the mutated enzyme variants, whereby substitutions of other positions had a destabilizing character [7]. Glycosylation site mutations of positions N13D and N268D in *E. coli* showed an increase in thermal and H_2O_2 stability and also changes of the kinetic parameters k_{cat} and K_M were observed, which were assigned to conformational changes of the enzyme molecule in this study [8].

1.1.6 Applications and production of HRP: state-of-the-art and purification issues

Horseradish peroxidase has been widely used in the field of biotechnology. Due to its high stability, catalytic activity and the ability to be easily conjugated to antibodies, the enzyme describes a useful tool for immunoassays and diagnostic kits, where it is mainly acting as an indicator by fluorescence, chemiluminescence or electrochemistry [9]. Another application is the treatment of industrial waste waters, because the enzyme is very stable in aqueous and

non-aqueous solutions, enabled via more stable enzyme variants that have been further improved by molecular biology techniques or chemical modifications (*vide supra*) [7, 8]. In organic chemical synthesis, HRP can be used for *N*- and *O*-dealkylation, oxidative coupling and much more catalysis-dependent reactions in this field [1]. In the last decades, HRP has attracted extensive research interest especially in the biopharmaceutical industry [5]. Together with indole-3-acetic acid (IAA), HRP is a high potential candidate for targeted cancer therapy. IAA derivatives can be oxidized by HRP, producing a cytotoxic substance for mammalian cells, not even requiring the presence of H_2O_2 for the formation of Compound I. IAA and HRP separated, are both not harmful for mammalians, which makes this system applicable for *in vivo* cancer therapies [10, 11].

According to this broad list of applications, there is an increasing demand for highly pure, but low-cost enzyme preparations. Authentic HRP is isolated from the horseradish root, which gives very low yields and results not in a single isoenzyme-preparation, but in a mixture of all isoenzymes present in the plant [1]. The purification from the horseradish root comprises ultrasonication, several precipitation steps and a more-dimensional chromatographic process, which makes the isolation from plant time-consuming and cost-intensive [12]. For this reasons, the enzyme was also expressed in different eukaryotic and prokaryotic recombinant host organisms. When recombinant horseradish peroxidase (rHRP) was produced in *E. coli* , the enzyme was found as inclusion bodies in a non-glycosylated form which required several laborious refolding steps, giving very low recovery yields [2]. Baculoviruses, mammalian and insect cell cultures were also used as a expression hosts, but the production was costly and yields were low [13, 14]. As another promising recombinant expression organism, yeasts such as *P. pastoris* and *S. cerevisiae* were used for the production of rHRP, resulting in hyperglycosylated enzyme species [15, 16]. The major disadvantage of these lower eukaryotic expression systems is the complication of a straight forward purification by conventional

chromatographic techniques, as the extensive glycosylation by the yeasts masks the physico-chemical properties of the enzyme and thus prevents interactions with the stationery phases [17]. The advantage of *Pichia* over *Saccharomyces* is that it adds less mannose residues to the glycan core as the baker's yeast (up to 100 Mannose units) [18, 19]. However, when HRP was expressed in *P. pastoris*, the molecular weight increased to approx. 65 kDa due to hypermannosylation (Figure 4). Details to the purification problem in the yeast *P. pastoris* are described in the first chapter of this thesis.

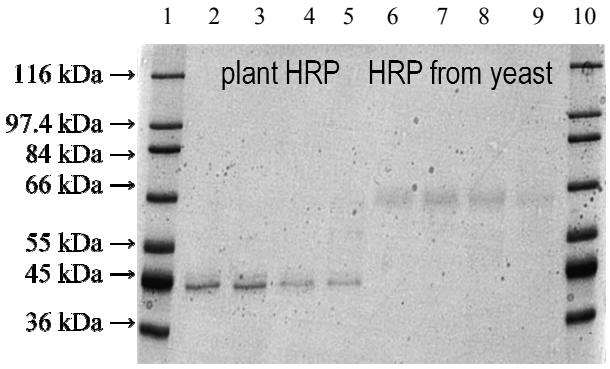

Figure 4: SDS-PAGE of HRP expressed in the plant and in *P.pastoris*. Lanes 1 and 10: molcular weight marker; lanes 2-5: HRP C from *A. rusticana*; lanes 6-9: rHRP expressed in *P. pastoris*.

Another problem is that the long mannose chains are antigenic when introduced intravenously into the human body, which is especially problematic when the enzyme should be applied for pharmaceutical purposes such as cancer therapies [10, 20]. However, *P. pastoris* appears as an auspicious host for the production of rHRP according to several advantages over other recombinant hosts, which are described in the following chapter.

1.2 *P. pastoris* as a recombinant host for heterologous protein production

1.2.1 History

Methylotrophic yeasts such as *P. pastoris* were used since the 1970s as an alternative to soybeans for the production of animal feeds due to the ability to utilize methanol as cheap sole carbon source. When the price for the plant source began to fall, methylotrophs were not competitive any more. In the 1980s, *P. pastoris* has attracted further research interest for heterologous protein expression, which was extensively investigated by a cooperation of the Phillips Petroleum Company and the Salk Institute Biotechnology/Industrial Associates, Inc. (SIBIA, La Jolla, CA) who established the *AOX*-promoter system and provided useful tools for the genetic manipulation of this yeast. This system was sold to SLR Research Corporation (Carlsbad, CA), who distributes the *P. pastoris* expression system since 1993 [20].

1.2.2 Methanol metabolism and heterologous protein expression

Methanol metabolism in *P. pastoris* relies on the presence of distinct enzymes, namely the two alcohol oxidase (AOX) enzymes which are present at substantial levels when the organism is grown on methanol. The methanol utilization pathway starts in the peroxisome with the conversion of methanol to formaldehyde and hydrogen peroxide by the AOX enzymes. The toxic byproduct H_2O_2 is degraded to water and oxygen by catalase, another enzyme present in the peroxisome. Parts of the generated formaldehyde leave the organelle and are converted to carbon dioxide and formate by dehydrogenases within the cytoplasm, a process maintaining energy metabolism. The remaining formaldehyde is degraded via another enzyme, dihydroxyacetone synthase (DHAS) forming a complex cylce of reaction steps. Both enzymes, AOX and DHAS are present in high levels during methanol growth, but not when

other carbon sources such as glycerol or glucose are utilized. Besides representing a cheap C-source, the growth on methanol has another advantagous effect; it also acts as an inducer for genes that are constituted after the *AOX*-promotors. In *P. pastoris*, there are two *AOX* genes present, *AOX1* and *AOX2*, whereby *AOX1* is the more dominant one and responsible for the majority of AOX-activity in the cell. The regulation of the *AOX*-promoters relies on a repression – derepression mechanism and an induction mechanism, whereby transcription is not detectable when a repressing carbon source such as glucose is absent. Thus, methanol is indispensable for induction of the *AOX*-promoters [20].

Another advantage of *P. pastoris* is the ease of genetic manipulation, which is quite similar to *S. cerevisiae*, the best characterized yeast species. *P. pastoris* can also integrate foreign genes via homologous recombination which are efficiently targeted to the *AOX1*-locus. This offers the advantage that any heterologous sequence can be transcribed from the genome of the host organism, not requiring any selection mechanism such as antibiotics resistance. Moreover, genomic integration provides highly stable expression strains which are superior to episomal vectors, notably not available for *P. pastoris* anyway [18].

Basically, there are three steps necessary for the expression of a foreign protein in *P. pastoris* [20]:

1. Insertion of the gene of interest into an appropriate expression vector (all vectors are designed as *E. coli – P. pastoris* shuttle vectors)
2. Introduction of the vector into the *P. pastoris* cell and integration into the genome
3. Selection of potential expression strains for heterologous protein production

A typical *P. pastoris* shuttle vector contains an origin of replication for plasmid maintainance and propagation in *E. coli*, a selectable marker such as antibiotics resistance (e.g. Zeocin® or Kanamycin) or auxotrophic markers (e.g. *HIS4* or *URA3*), 5‘ *AOX*-promoter sequences and a

short sequence for transcript-termination. Of course, multiple cloning sites for the insertion of the gene of interest are present. An additional feature is a secretion signal for extracellular expression, the *S. cerevisiae* α-mating factor (also referred to as alpha pre-pro signal sequence) being the most popular one.

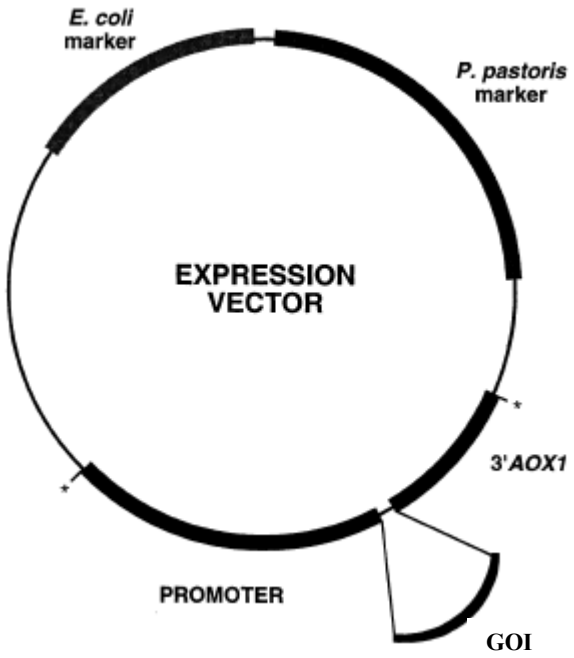

Figure 5: A typical *P. pastoris* expression vector [20]. The expression cassette contains an *AOX* promoter and terminator and selection markers for *P. pastoris* as well as for *E. coli* . The gene of interest (GOI) is inserted between the *6* elements.

1.2.3 Phenotypes of *P. pastoris* strains, cultivation conditions and glycosylation

There are three defined types of strains for heterolgous protein expression available, which differ in their ability to metabolize methanol. The most popular one, Mut^+ (**m**ethanol **ut**ilization **plus**) grows on methanol at the wild-type rate, as these strains keep both native *AOX* genes. There are strains available, where one of the *AOX* genes is deleted, resulting in slow methanol-utilization rates because alcohol metabolism is relying on the weaker *AOX2* promoter. These types of strains are referred to as Mut^S (**m**ethanol **ut**ilization **s**low) strains. A major advantage of Mut^S strains is that they require less methanol for growth as Mut^+ strains and can also yield in higher levels of heterologous protein. Furthermore, Mut^+ strains need less oxygen and thus produces less heat. The third class of *P. pastoris* strains is called Mut^- (**m**ethanol **ut**ilization **minus**) where both *AOX* genes are deleted and the cells are totally unable to grow on methanol. However, all three strains induce heterologous protein expression when methanol is present. There are also some protease-deficient strains available, such as SMD1168H resulting in reduced degradation of foreign proteins by endogenous proteases, but these strains are not as viable and efficient in methanol utilization as wild-type strains and furthermore, they are more difficult to transform [20].

The yeast *P. pastoris* has a preference for respiratory growth, which allows the cultivation at very high cell densities resulting in high product titers. This is especially true when the culture is fed methanol at growth-limiting rates. Moreover, methanol metabolism requires high levels of oxygen which is why the best cultivation conditions can be achieved in bioreactors rather than in shake flasks. Usually, cells are grown on defined glycerol or glucose media for biomass accumulation. After the depletion of the repressing substrate, a transition phase at growth-limiting glycerol rates is performed before the culture is induced by methanol and heterologous protein expression is started. *P. pastoris* is perfectly suitable for large-scale

production of foreign proteins because the required media are cheap and simple and no toxins are present in the fermentation broth. Another benefit is the ability to secrete foreign proteins into the fermentation broth, representing the vast majority of the extracellular protein content because *Pichia* secretes only very low levels of endogenous proteins. The first step in purification is then simply the removal of the biomass rather than recovering the product from the intracellular space or from inclusion bodies.

The major advantage of *P. pastoris* over prokaryotic expression systems such as *E. coli* is the fact that it is capable of performing post-translational modifications such as proteolytic processing, folding, disulfide bridge formation and glycosylation. *Pichia* can perform *N*- and *O*-linked glycosylation. *O*-oligosaccharides comprise only mannose residues, but little is known about the detailed mechanism of *O*-glycosylation in *P.pastoris*. However, it seems that there is no clear consenus-sequence yet defined for the recognition of *O*-glycosylation sites. On the other hand, *N*-glycosylation sites are recognized by the consensus sequence Asn-X-Ser/Thr, whereby X must not be Proline. Starting from this point, the core structure $Man_8GlcNAc_2$ is synthesized to the Asparagine residue in the Endoplasmatic Reticulum. In the Golgi apparatus, the final oligosaccharide composition of $Man_{5-6}GlcNAc_2$ (also referred to as „high mannose type“) is generated. *P. pastoris* elongates the N-linked core unit of secreted proteins with several mannose residues. No terminal α-1,3-linked mannose residues have been reported [21], but α-1,6-linkages on core-related structures were described, *e.g.* [22].

Yeasts such as *P. pastoris* or *S. cerevisiae* are also capable of phosphorylating proteins in the form of mannose-I-phosphate at specific α-1,2- or α-1,6-linked mannose residues, altering thereby the acidity of the native protein [19].

The above listed advantages, the availability of engineered host strains and plasmids and the *in-house* knowledge of this yeast made the *Pichia* expression system a suitable host for the recombinant production of HRP C within this thesis.

1.3 Motivation and Goals

As depicted above, HRP represents a very important enzyme for industry as well as for medicine and thus, it is obvious that there is a high demand of pure, homogeneous and economic enzyme preparations. Many efforts have been made to produce HRP recombinantly in different hosts, but a range of issues have not been solved yet to make this processes competitive to HRP extraction from plant.

Yeasts that produce high titers of a recombinant product tend to hyperglycosylate the target protein, which also raises the cost of production as the downstream processing of hyperglycosylated proteins is significantly impaired. Efficient strategies need to be developed in order to obtain cost-reduced and well defined enzyme preparations that can be selected according to their intended use. Thus, this thesis aims to develop a fast and economic purification strategy for recombinant hyperglycosylated HRP produced in *P. pastoris*, necessary for the production of cost-efficient HRP enzyme preparations that are comparable to commercially available HRP and that can be applied in industry and medical diagnostics. As there is a hole range of other HRP isoenzymes identified but no purification strategy yet developed, this may also be interesting in a wider perspective.

The first part of this thesis introduces the purification problem of rHRP produced in *P. Pastoris* and describes a straight forward purification strategy. After performing univariate experiments, a multivariate approach using Design of Experiments optimizes the 2-step purification protocol and gives outlook to future applications.

Especially for *in vitro* use in medical applications such as targeted cancer therapies, less- or non-glycosylated forms of HRP are required but are not yet available on the market. Hence, the second goal of this thesis is to reduce the glycosylation pattern of rHRP in a molecular

biology approach and express it in *P. pastoris* with at least same catalytic and thermal stability as the wild type enzyme isolated from plant. Therefore, one of the 9 glycosylation sites will be replaced by three structural similar amino acids using splicing-by-overlap-extension PCR. The most promising enzyme variants will be expressed in a larger scale and thoroughly charactarized using biochemical tests and mass spectrometry.

Here, a from-start-to-finish protocol should be established in order to remove all potential glycosylation sites of rHRP in the future.

This thesis provides solid information about the purification of hyperglycosylated recombinant proteins produced in *P. Pastoris,* opens a way to reduce the glycosylation pattern of rHRP and the generated enzyme variants are characterized in detail. Finally, both parts are resumed in the overall conclusions chapter and an future perspectives are discussed.

2 Purification studies of recombinant horseradish peroxidase expressed in *P. pastoris*

Parts of this worked were published recently:

Rossetti L., Spadiut O., Dietzsch C., Herwig C., Purification of a recombinant plant peroxidase produced in *P. pastoris* by a simple 2-step strategy; *Protein Expression and Purification* 86 (2012) 89-97

2.1 Introduction

Due to the emerging number of medical and industrial applications of HRP, there is an increasing demand for highly pure, but low-cost enzyme preparations. In this respect, several different host organisms for the production of the enzyme were tested. Numerous publications have reported the functional expression of rHRP in yeasts like *P. pastoris* [15, 16, 23-25]. In all these studies, the authors described hyperglycosylation of the produced rHRP by the yeast, a phenomenon which is known for this expression host [26], resulting in an enzyme preparation with a molecular mass of around 65 kDa [23] [15, 16, 24, 25]. This extensive glycosylation pattern apparently masks the physico-chemical properties of rHRP hampering a fast and efficient downstream process [15]. However, as shown by Tams and Welinder [5], a simple enzymatic deglycosylation of the enzyme is not possible. Hence, established processes for the purification of rHRP from yeast comprise several steps and are quite cumbersome (Table 1; [15]). Since it is possible to purify HRP from plant by a single affinity chromatography step employing the lectin concanavalin A (Table 1, [27, 28]), the enzyme is still mainly isolated directly from the horseradish root. However, lectin-carrying resins are comparatively expensive and can not be used frequently without experiencing a loss in

binding capacity. Thus, also other strategies to purify HRP from plant have been developed, but several steps are required to obtain purified enzyme and recovery yields are low (Table 1).

Table 1: Purification strategies for glycosylated HRP produced in different host organisms.

host	purification strategy	recovery yield	reference
yeast	ammonium sulphate precipitation, hydrophobic interaction chromatography, gel filtration, anion exchange chromatography	n.m.	[15]
horseradish	affinity chromatography	73 %	[29]
horseradish	affinity chromatography in an aqueous two-phase system	60%	[30]
horseradish	membrane affinity chromatography	25 %	[31]
horseradish	affinity chromatography	73 %	[27]
horseradish	ultrasonication, ammonium sulphate precipitation, hydrophobic interaction chromatography	71 %	[12]
horseradish	ammonium sulphate precipitation, anion exchange chromatography, gel filtration	< 20 %	[32]

n.m. not mentioned

Another problem regarding HRP from plant is that the enzyme exists in different isoforms which are tricky to separate from each other. Besides, the amount of enzyme in the plant is low. Lavery *et al.*, for example, only obtained around 10 mg of purified HRP out of 100 g

horseradish roots [12]. Hence, it would be advantageous to produce the desired HRP isoenzyme recombinantly and to purify it in a simple and cost-effective way.

The first part of this thesis comprised the development of fast and efficient 2-step purification protocol for recombinant hyperglycosylated horseradish peroxidase expressed in *P. pastoris* .

2.2 Material and Methods

2.2.1 Processing the fermentation broth

After harvesting the fermentation broth from different dynamic fed-batch experiments [16, 33], the solution was centrifuged (5,000 rpm, 4°C, 20 min) and the supernatant was concentrated between 15- and 20-fold and the buffer was exchanged dependent on the subsequent purification strategy (Table 2) by diafiltration using a 10 kDa cut-off membrane (Omega T-series; PALL, Austria). Diafiltration was performed at room temperature with a total filter area of 0.3 m^2 and a max. flowrate of 2.4 L/min using the crossflow filtration system Centramate 500S (PALL). During diafiltration, the transmembrane pressure was kept below 1 bar not to harm the enzyme. Before the crude extract was loaded onto the respective chromatography resin, it was filtered through a 0.2 µm cut-off filter (GE Healthcare, Sweden).

2.2.2 Enzymatic activity and protein concentration

The enzymatic activity of HRP was determined using a CuBiAn XC photometric robot (OptoCell, Germany). Samples (10 µl) were added to 140 µl of 1 mM ABTS (2.2' azino bis 3-ethylbenzthiazoline-6-sulphonic acid) in 50 mM KH_2PO_4 buffer (pH 6.5). The mixture was incubated at 37°C and the reaction was started by the addition of 20 µl of 0.075 % (v/v) H_2O_2. Changes of absorbance at 415 nm were measured for 80 seconds and rates were calculated.

Calibration was done with commercially available HRP (Sigma-Aldrich) at six different concentrations (0.02-2.0 U/mL). Protein concentrations were determined at 595 nm by the Bradford assay (M.M., 1976) using the BioRad Protein Assay Kit with bovine serum albumin (BSA) as standard in the range of 0.2-1.2 mg/mL using a Hitachi U-1100 spectrophotometer (Hitachi, Germany).

2.2.3 Screening of different purification strategies

All chromatography purification runs were performed at room temperature on an ÄKTApurifier^{TM} system (GE Healthcare). For affinity chromatography (AC), hydrophobic interaction chromatography (HIC), cation exchange chromatography (CEX), anion exchange chromatography (AEX) and hydrophobic charge induction chromatography (HCIC) different resins were packed manually in a HiScale^{TM} 16/20 column (GE Healthcare) to a final column volume of approx. 20 mL packed bed. The chromatographic media used for AC, HIC, CEX and AEX were from GE Healthcare and the MEP HyperCel resin used for HCIC was from PALL. The total protein concentration of the crude extract was 0.4 mg/mL. For all chromatography runs the amount of protein loaded onto the resin was between 5- and 10-fold below the maximum binding capacity of the respective resin. On average, between 40-60 mg of total protein were applied per purification run. Before loading, the resin was equilibrated with at least 5 column volumes (CV) of binding buffer. A post-load wash of 4 CV binding buffer was performed, before the retained proteins were eluted in a linear gradient of 0-100 % elution buffer within 5 CV, unless otherwise stated. The resins, enzyme preparation, buffer compositions and flow rates used in this study are summarized in Table 2**Table 2**. Buffers were prepared using chemicals of reagent grade (Sigma–Aldrich, Germany) and filtered through a 0.2 μm cut-off filter before use.

2.2.4 CIM monolithic columns as a potential second step

Univariate screenings for a potential application of CIM monolithic columns as a second chromatographic purification step were performed with either partially HCIC-purified rHRP or with cell-free supernatant from *P. pastoris* shake flask experiments or bioreactor cultivations. Crude fermentation supernatant or flowthrough fractions from HCIC purifications were pooled, concentrated and rebuffered in the respective loading buffer: 50 mM Tris-Cl pH 7.4 or pH 8.0, 50 mM KH_2PO_4 pH 6.0; elution buffers included 1 M Sodium-chloride. The monolithic columns were 1 mL CIM-DEAE, CIM-QA or CIM-OH (BiaSeparations, Slovenia) with one column volume (CV) of 1 mL, which were washed with 10 CV of deionized water, pre-equilibrated with 10 CV of each, loading and elution buffer at half of the working flowrate (2 mL/min) followed by a 20 CV equilibration step in loading buffer at a working flowrate (4 mL/min). For loading, flowrates varied from 0.5 – 2 mL/min. A post load wash of 4 CV binding buffer was performed before elution in different profiles was conducted by either increasing the high-salt elution buffer a) stepwise, b) in a linear gradient to 100% B in 30 CV or c) in a combination of both.

2.2.5 Salt precipitation

Besides screening different chromatography techniques, we also tried the more traditional strategy of salt precipitation to purify rHRP. For this purpose, we either used $(NH_4)_2SO_4$ or Na_2SO_4 [34] and stepwise added the corresponding amount of salt to the crude extract (stepsize: 0/20/40/60/80/100 %) to a final concentration of 5 M $(NH_4)_2SO_4$ and 1.2 M Na_2SO_4, respectively. After each salt addition, the solution was stirred at 4°C for at least 1 hour to obtain equilibrium. The solution was centrifuged (5,000 rpm, 30 min) to harvest precipitated proteins, which were then resuspended in 2 mL KH_2PO_4 buffer (50 mM, pH 6.5). The catalytic activity and protein concentration of the resuspended precipitates and the corresponding supernatants were measured.

Size-exclusion chromatography (SEC) was performed using a prepacked HiLoad™ 16/600 Superdex™ 75 pg column (GE Healthcare). For SEC runs, we used centrifugal filter units (Ultracel-30K; Millipore, Ireland) to concentrate partially purified protein solutions to a concentration of 5.0 mg/mL and applied 1 mL thereof to the equilibrated SEC column.

Table 2: Purification principle, resin, HRP source, buffer compositions and flow rates applied in this study.

principle	resin	expression host	binding buffer	elution buffer	flow rate [cm/h] load/elution
AC	ConA Sepharose 4B	Plant	50 mM TrisHCl, 1 mM $CaCl_2$, 1 mM $MnCl_2$, 1 mM $MgCl_2$, 500 mM NaCl, pH 7.4	100 mM NaAc, 1 M α-D-Methylmannoside, pH 5.5	60/60
		P. pastoris	50 mM TrisHCl, 1 mM $CaCl_2$, 1 mM $MnCl_2$, 1 mM $MgCl_2$, 500 mM NaCl, pH 7.4	100 mM NaAc, 1 M α-D-Methylmannoside, pH 5.5	
			50 mM citrate, 1 mM $CaCl_2$, 1 mM $MnCl_2$, 1 mM $MgCl_2$, 500 mM NaCl, pH 6.5	100 mM citrate, 1 M α-D-Methylmannoside, pH 5.5	
HIC	Phenyl Sepharose HP	*P. pastoris*	50 mM KH_2PO_4, 1 M $(NH_4)_2SO_4$, pH 6.5	50 mM KH_2PO_4, pH 6.5	60/120
CEX	SP Sepharose FF	*P. pastoris*	20 mM citrate, pH 4.0	20 mM citrate, 1 M NaCl, pH 4.0	60/120
	Capto S	*P. pastoris*	20 mM acetate, pH 4.0	20 mM acetate, 1 M NaCl, pH 4.0	

AEX	Q Sepharose FF	*P. pastoris*	20 mM BisTris, pH 6.0	20 mM BisTris, 1 M NaCl, pH 6.0	60/120
			20 mM BisTris, pH 7.0	20 mM BisTris, 1 M NaCl, pH 7.0	
	Capto Q	*P. pastoris*	20 mM BisTris, pH 7.0	20 mM BisTris, 1 M NaCl, pH 7.0	
HCIC	MEP HyperCel	*P. pastoris*	50 mM TrisHCl, 1 M NaCl, pH 8.0	50 mM NaAc, pH 4.0	60/60
			20 mM NaAc, 500 mM NaCl, pH 4.5*	50 mM TrisHCl, pH 8.0	
SEC	Superdex 75	*P. pastoris*	50 mM KH_2PO_4, 150 mM NaCl, pH 6.5		9
					18
					27
CIM-monolithic columns	DEAE-1	*P.pastoris*	50 mM Tris-Cl, pH 8.0	50 mM Tris-Cl, 1 M NaCl pH 8.0	0.5 mL/min
					1 mL/min
					2 mL/min
			50 mM Tris-Cl, pH 7.0	50 mM Tris-Cl, 1 M NaCl pH 7.0	0.5 mL/min
					1 mL/min
					2 mL/min
			50 mM NaAc, pH 6.0	50 mM NaAc, 1 M NaCl pH 6.0	0.5 mL/min
					1 mL/min
	OH		20 mM NaAc, pH 4.5 + 3 M NaCl	20 mM NaAc, pH 4.5	2 mL/min
	QA-1		50 mM Tris-Cl, pH 8.0	50 mM Tris-Cl, 1 M NaCl pH 8.0	1 mL/min

*a post-load low-salt wash with 5 CV of 20 mM NaAc,150 mM NaCl, pH 4.5 was performed before elution

2.2.6 Screening for significant factors influencing the purification performance by a multivariate Design of Experiments

2.2.6.1 HCIC

We performed a multivariate Design of Experiments (DoE) screening study to determine parameters, which significantly influence the performance of HCIC. A HiScale 16/20 empty column was manually packed with MEP HyperCel resin using 1M NaCl in 20% EtOH, as recommended by the supplier. After equilibration with 5 CV of the same solution, 0.05 % CV of 5 % actone (v/v) was injected to determine column performance parameters. This procedure was repeated three times. The number of theoretical plates per meter (N/m) and the asymmetry factor (AF) were automatically calculated by the Unicorn® software (GE Healthcare) according to equations 2 and 3.

$$\frac{N}{m} = \frac{5.54 \cdot {t_R}^2}{d^2 \cdot L} \qquad \text{(Equation 2)}$$

$$AF = \frac{b}{a} \qquad \text{(Equation 3)}$$

, where t_R is the retention volume (mL), d the peak width at half height (mL), L the column length (in cm for HETP, in m for N/m) and a and b the left and right distance from peak centre at 10 % peak height, respectively.

A 2-level cubic full factorial screening approach with 3 centre points was set up with the program MODDE (Umetrics AG, Umea, Sweden) to explore the influence of the factors "flow rate" (50-100 cm/h), "ionic strength of the equilibration buffer" (0-1 M NaCl) and "pH of the equilibration buffer" (pH 4.0-6.0) as well as their linear interactions on the response parameters "specific activity" and "recovery yield" of the total flowthrough and "purification factor" of single flowthrough fractions (Table 3). Fraction size was chosen with 5 mL.

Table 3: Worksheet for the multivariate factor screening approach for HCIC using the program MODDE. The response parameters were "specific activity" and "recovery yield" of the total flowthrough and "purification factor" of single flowthrough fractions.

Exp No	Run Order	flow rate [cm/h]	NaCl [M]	pH
1	10	50	0	4
2	2	100	0	4
3	5	50	1	4
4	11	100	1	4
5	1	50	0	6
6	8	100	0	6
7	6	50	1	6
8	9	100	1	6
9	7	75	0.5	5
10	3	75	0.5	5
11	4	75	0.5	5

2.2.6.2 SEC

All SEC runs in this study were performed with a prepacked HiLoad™ 16/600 Superdex™ 75 pg column (GE Healthcare). The number of theoretical plates per meter was given with N > 13,000 m^{-1} by the supplier. Again a 2-level cubic full factorial screening approach was set up to explore the influence of the factors "flow rate" (9.0-45.0 cm/h) and "sample volume" (0.5-5.0 mL) as well as their linear interactions on the response parameters "purification factor" and "recovery yield" of single fractions (Table 4). Fraction size was chosen with 2 mL.

Table 4: Worksheet for the multivariate factor screening approach for SEC using the program MODDE. The response parameters were "purification factor" and "recovery yield" of single fractions.

Exp No	Run Order	flow rate [cm/h]	sample volume [mL]
1	5	9	0.5
2	1	45	0.5
3	6	9	5
4	3	45	5
5	2	27	2.75
6	4	27	2.75

2.2.7 Data analysis

To evaluate the success of purification steps, the enzymatic activity [U/mL] and the protein concentration [mg/mL] in the crude extract, the flowthrough fractions and the eluted fractions were measured and the respective specific activities [U/mg] were determined. The specific activity of the crude extract was compared to those of the fractions and the purification factor (PF) was calculated (Equation 4).

$$PF = \frac{specific\ activity_{\ fraction}}{specific\ activity_{\ crude\ extract}} \qquad \text{(Equation 4)}$$

To check for possible losses and potential denaturation of the enzyme during the process, the recovery yield of the catalytic activity (Y_A) and the protein concentration (Y_P), *i.e.* whether all Units and the total amount of protein was recovered in the sum of the flowthrough and all eluates, were calculated according to Equations 5 and 6.

$$Y_A[\%] = \left(\frac{(catalytic\ activity\ _{fractions} + catalytic\ activity\ _{flowthrough}}{catalytic\ activity\ _{crude\ extract}} \right) \cdot 100 \qquad \text{(Equation 5)}$$

$$Y_P[\%] = \left(\frac{(protein\ concentration\ _{fractions} + protein\ concentration\ _{flowthrough}}{protein\ concentration\ _{crude\ extract}} \right) \cdot 100 \qquad \text{(Equation 6)}$$

2.2.8 Electrophoresis

To check the purity of rHRP and the presence of contaminating proteins, electrophoresis was done. SDS-PAGE was performed using a 5 % stacking gel and a 10 % separating gel in 1x Tris-glycine buffer. Unless otherwise stated, samples were diluted to a protein concentration between 0.5-1.0 mg/mL before loading. Gels were run in a vertical electrophoresis Mini-PROTEAN Tetra Cell apparatus (Biorad, Austria) and stained with Coomassie blue. The protein mass standard used was the PageRuler Prestained Ladder (Fermentas, Austria).

Isoelectric focussing was carried out with pre-cast Novex® IEF Gels pH 3-10 (Invivogen, USA). The runs were performed according to the Novex® IEF Gels quick reference guide. Gels were stained with Coomassie colloidal staining solution or silver stain. Protein amounts loaded onto the gel cassette varied between 10 and 22 µg per lane. The IEF marker used was the Serva Liquid Mix (Serva Electrophoresis, Germany) in the range from pI 3.5 to 10.7.

2.3 Results and Discussion

2.3.1 Crude extract and pH stability of HRP

A recombinant *P. pastoris* strain was cultivated in fed-batch fermentations [33] and the fermentation broths were processed to obtain a cell-free crude extract with a specific activity of around 80 U/mg. Recombinant HRP was produced extracellularly by *P. pastoris*, which facilitated processing of the fermentation broth. However, also different other proteins were secreted by *P. pastoris*, as described in detail recently [35] and shown in Figure 8, Figure 9 and Figure 11 underlining the need for an efficient purification strategy for rHRP.

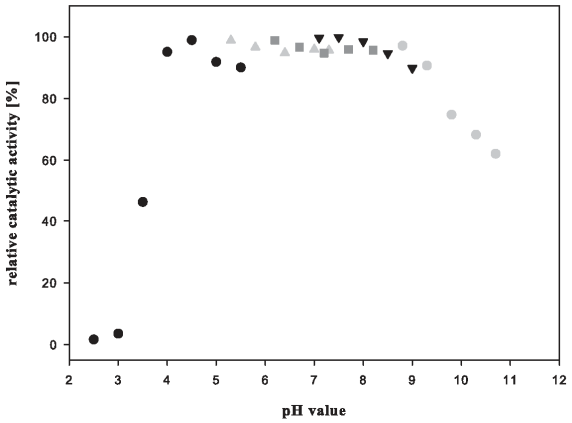

Figure 6: pH stability of HRP isolated from plant containing approx. 70 % isoenzyme C [15, 36]. HRP was incubated in different 50 mM buffers at 30°C for 30 min before the remaining enzymatic activity was determined photometrically. ●, citrate-buffer; ▲, carbonate-buffer; ■, phosphate-buffer; ▲, Tris-buffer; ●, glycine-buffer.

The stability of HRP was determined with univariate experiments between pH 2.5-10.7. As shown in Figure 6, HRP showed high stability between pH 4.0 and 9.0. Only at lower and higher pH values a significant reduction of the enzymatic activity was observed.

2.3.2 Univariate screening of different purification strategies

We screened different methods to identify promising purification strategies for rHRP from *P. pastoris*. In general, for all purification runs performed values for both Y_A and Y_P were between 94-100 %. Thus, we assumed that no protein was lost and rHRP was not denatured during the different processes.

2.3.3 Affinity chromatography AC

The lectin concanavalin A (ConA) specifically binds glucose- and mannose-units and was used to purify glycoproteins before (e.g. [27, 28, 37]). We used a ConA resin to purify HRP isolated from plant (commercial enzyme preparation from Sigma-Aldrich, P6782-100MG), containing approx. 70 % isoenzyme C [15, 36], and the hyperglycosylated rHRP from *P. pastoris*.

The purification of the plant enzyme was straightforward, as the enzyme bound to the ConA resin with only very little amount of enzyme found in the flowthrough (< 4 %), and eluted at a concentration of around 0.5 M α-D-Methylmannoside (Figure 7A). On the contrary, the hyperglycosylated enzyme produced in *P. pastoris*, even though carrying much more mannose units on its surface, did not bind to the ConA resin independent of the buffer and pH value applied (Figure 7B).

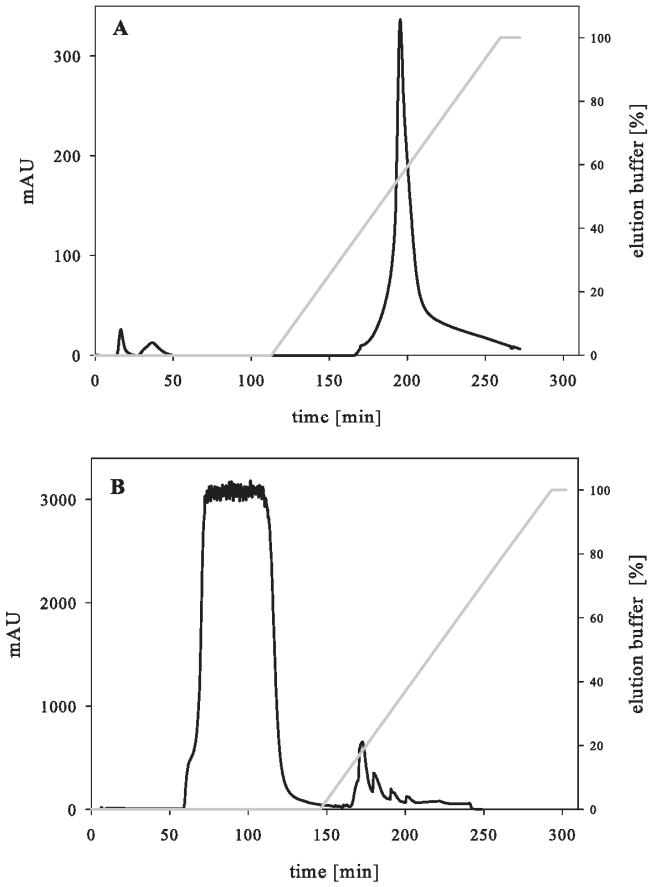

Figure 7: Chromatograms of affinity chromatography runs with HRP and a ConA resin. A) HRP from plant; B) hyperglycosylated rHRP produced in *P. pastoris*. Black line, UV-signal A_{280}; grey line, gradient of elution buffer (containing 1 M α-D-Methylmannoside).

Only a minor amount of rHRP was retained on the stationary phase (< 5 %). Surprisingly, the extensive glycosylation pattern of rHRP somehow prevented the interaction between the carbohydrates on the surface of the enzyme and the lectin, whereas the less glycosylated enzyme isolated from plant was retained. We currently have no explanation for this unexpected result. However, due to high costs of α-D-Methylmannoside, especially with regard to a possible scale-up, and due to the fact that the resin can only be used for a limited number of purification runs before experiencing a loss in binding capacity, we decided not to investigate this purification principle further.

2.3.4 Salt precipitation

Since affinity chromatography was not successful, we tried to partially purify rHRP by salt precipitation, a technique commonly used in combination with a subsequent HIC step (e.g. [34]). We calculated the net charge of rHRP without the signal sequence with -2.9 and thus expected poor water solubility of the enzyme (HydrophobicityPlotter; Innovagen, Sweden; http://www.innovagen.se/).

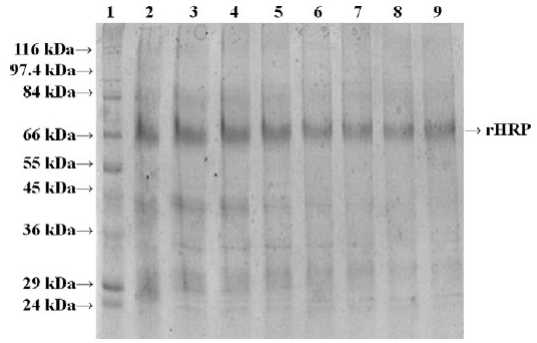

Figure 8: SDS-PAGE of fractions obtained during $(NH_4)_2SO_4$ precipitation of rHRP. Lane 1, molecular mass standard; lane 2, crude extract (5 µg); lane 3, crude extract (10 µg); lane 4-8, precipitates at 1/2/3/4/5 M $(NH_4)_2SO_4$ (between 5-7 µg); lane 9, supernatant at 100 % $(NH_4)_2SO_4$ (5 µg).

However, when we used $(NH_4)_2SO_4$ to precipitate rHRP, we actually found more than 75 % of the enzyme still in solution at a concentration of 5 M salt. The other 25 % of the enzyme were found distributed in all the precipitates from 1-5 M $(NH_4)_2SO_4$ (Figure 8), indicating the presence of a variety of differently glycosylated enzyme species. Contrary to the prediction, hyperglycosylated rHRP exhibited a very high affinity to H_2O, most probably due to the extensive glycosylation pattern.

Interestingly, the specific activity of rHRP in the supernatant at a concentration of 5 M $(NH_4)_2SO_4$ was 3-fold higher than in the crude extract (86 U/mg in the crude extract vs. 275 U/mg in the supernatant). By precipitating contaminating proteins, we achieved a purification factor (PF) of 3, but also lost around 25 % of rHRP as precipitates. However, salting out contaminating proteins could be a valuable strategy to partially purify the apparently

hydrophilic rHRP without great losses. We obtained very similar results when we used Na_2SO_4 instead of $(NH_4)_2SO_4$.

2.3.5 Hydrophobic interaction chromatography HIC

Since we were able to salt out the more hydrophobic contaminating proteins in salt precipitation experiments, we wanted to apply basically the same principle using a chromatography method. When we loaded the diafiltrated crude extract to a HIC column in the presence of 1 M $(NH_4)_2SO_4$ (Table 2), we found more than 80 % of rHRP in the flowthrough, whereas a lot of contaminating proteins were retained on the resin. We repeated this experiment three times and always observed PFs of at least 2.0 in the flowthrough, which shows the possibility of using this flowthrough strategy to partially purify rHRP. However, around 20 % of rHRP bound to the HIC resin and could not be recovered in the flowthrough.

2.3.6 Cation exchange chromatography CEX

We calculated the theoretical isoelectric point (pI) of unglycosylated rHRP without the signal sequence with 6.4 (ExPASy; http://web.expasy.org/). However, when we performed isoelectric focussing (IEF) with partially purified rHRP after HIC runs, we observed several intensive bands with pIs between 3.5-5.0. Due to the pH stability of plant HRP (Figure 6), we decided to use buffers with a pH value greater than pH 4.0 for CEX chromatography runs to avoid possible denaturation of rHRP. For both resins and buffer systems tested (Table 2), we did not observe any binding of rHRP. At pH 4.0, rHRP was either not charged enough or the extensive glycan pattern on the surface of the enzyme masked its physico-chemical properties preventing a charged-based interaction with the stationary phase. However, some contaminating proteins bound to the CEX resins resulting in a PF of around 1.5 in the flowthrough.

2.3.7 Anion exchange chromatography AEX

Since we determined several apparent pIs between 3.5 and 5.0 for rHRP, we used buffers with pH values of 6.0 and 7.0 to obtain charged rHRP for AEX experiments. When Q Sepharose FF was used at pH 6.0 and 7.0, 60-65 % of rHRP but only around 20 % of the total protein content were found in the flowthrough, resulting in a PF of 3.1 and 3.5, respectively.

When Capto Q was used as AEX resin at pH 7.0, around 50 % of rHRP and 12 % of the total protein content were found in the flowthrough giving an even higher PF of around 4.0 (Figure 9).

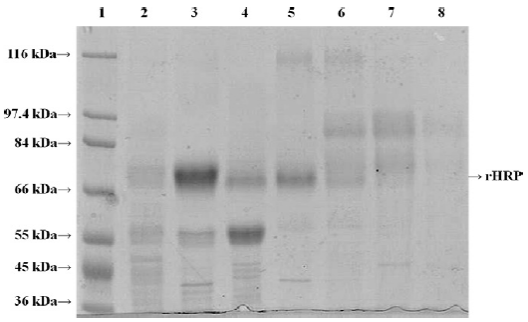

Figure 9: SDS-PAGE of fractions from AEX with rHRP at pH 7.0 using a Capto Q resin. Lane 1, molecular mass standard; lane 2, crude extract (4 µg); lane 3, flowthrough (10 µg); lane 4-8, fractions eluted at increasing concentrations of NaCl (between 2-10 µg).

However, around 50 % of rHRP bound to the resin and eluted at increasing salt concentrations concomitantly with other proteins. This again indicates that rHRP does not describe a single defined species with a homogenous glycosylation pattern, but rather a variety of species carrying different glycan chains. This is also depicted in SDS gels, where rHRP appears as a smear at around 60-70 kDa rather than a descrete band (Figure 8, Figure 9 and Figure 11; [15, 16]). Summarizing, an AEX purification step operated in flowthrough mode gave a quite high PF of around 4.0 for hyperglycosylated rHRP, but up to 50 % of the enzyme bound to the resin and were not recovered in the flowthrough. All AEX screening runs were repeated at least twice to check for reproducibility.

2.3.8 Hydrophobic charge induction chromatography HCIC

Hydrophobic charge induction chromatography (HCIC) describes a bimodal chromatography principle in which proteins bind due to hydrophobic interactions. Desorption is based on ionic charge repulsion by changing the pH value of the mobile phase. In contrast to traditional HIC, HCIC is controlled on the basis of both pH and salt concentration. For this study, we chose a HCIC resin carrying the ligand 4-mercapto-ethyl-pyridine (MEP) with a pKa of 4.8. We tested the potential interaction of rHRP with the HCIC resin at both alkaline and acidic pH values (Table 2).

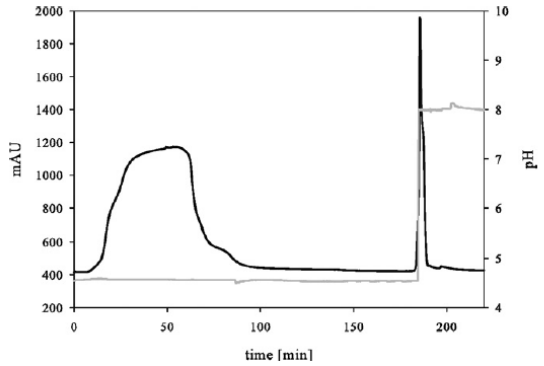

Figure 10: Chromatogram of a HCIC run with rHRP. Instead of a gradient elution, a step-wise elution from 0 – 100 % elution buffer was performed. Black line, UV signal; grey line, pH value.

At pH 8.0 neither rHRP nor contaminating proteins bound to the resin. Using an alternative binding buffer at pH 4.5 containing a moderate salt concentration, rHRP did again not bind to the resin as 93 % of the enzyme were found in the flowthrough. However, contaminating proteins were retained on the stationary phase (Figure 10).

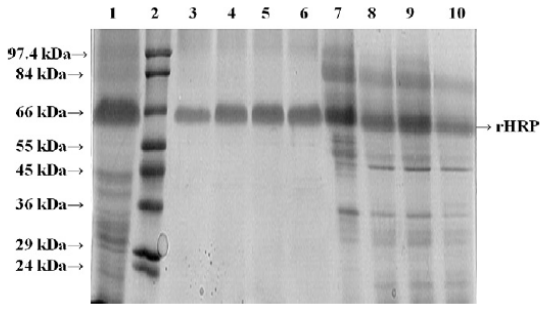

Figure 11: SDS-PAGE of fractions from HCIC with rHRP and a MEP HyperCel resin. Lane 1, crude extract (10 µg); lane 2, molecular mass standard; lanes 3-6, flowthrough fractions (5 µg); lanes 7-10, eluted fractions (10 µg).

At pH 4.0 the MEP ligand is positively charged and apparently a lot of contaminating protein in the fermentation broth of *P. pastoris* are negatively charged and retained due to ionic interactions. In contrast, the extensive glycosylation pattern of rHRP masks the physico-chemical properties of the enzyme, which is why rHRP did not interact with the resin independent on the pH value of the binding buffer. Since the majority of rHRP was found in the flowthrough, we could shorten the process time by skipping the post-load low-salt wash and by applying the fermentation broth directly to the resin without diafiltration.

Summarizing, using a binding buffer at pH 4.5 contaminating proteins were retained and the resulting rHRP preparation in the flowthrough was 5.0-fold purified to a specific activity of more than 400 U/mg (Figure 11).

2.3.9 Size exclusion chromatography SEC

We used SEC to polish partially purified rHRP preparations. We used flowthrough fractions of rHRP after AEX (Capto Q, pH 7.0; PF ~ 4.0), concentrated the protein solution to approx. 5.0 mg/mL by ultrafiltration and loaded 1 mL thereof on a prepacked Superdex 75 column (GE Healthcare) at different flow rates (Table 2).

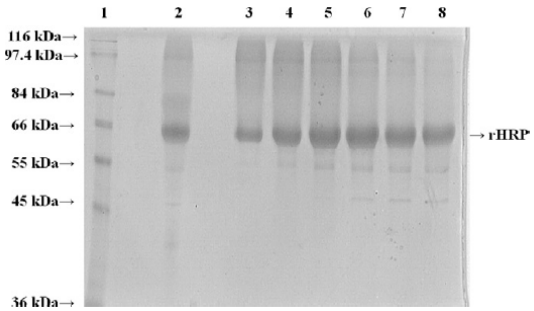

Figure 12: SDS-PAGE of fractions from SEC of partially purified rHRP after AEX with a flow rate of 18 cm/h. Lane 1, molecular mass standard (5 µg); lane 2, partially purified rHRP after AEX (5 µg); lane 3-8, eluted fractions of SEC (between 5 - 7 µg).

Independent on the flow rate applied we observed a PF between 2.0 and 2.5 (Figure 12; lane 2, partially purified rHRP after AEX: 340 U/mg; lane 3, fraction of SEC: 750 U/mg). All SEC runs were performed at least twice to check for reproducibility. Table 5 summarizes all purification strategies that were tested in a univariate manner and presents their respective prufication factors and recoveries.

Table 5: Summary table of strategies to purify hyperglycosylated rHRP produced in *P. pastoris*.

principle/resin	operation mode	PF	recovered rHRP [%]
salt precipitation	rHRP in solution at 5 M salt	≥ 3.0	75
HIC/Phenyl Sepharose	flowthrough	≥ 2.0	80
CEX/SP Sepharose	flowthrough	1.5	100
AEX/CaptoQ	flowthrough	4.0	50
HCIC/MEP HyperCel	flowthrough	5.0	93
SEC/Superdex 75	standard	≥ 2.0	100

2.3.10 Screening for significant factors influencing the purification performance by a multivariate Design of Experiments

HCIC

In the univariate screening study, we determined a HCIC operated in flowthrough mode to give the highest PF and a recovery yield of more than 90 % (Table 5). To obtain more information on this system and to find the optimal operation conditions, we analyzed possible influences of the three factors "flow rate", "ionic strength of the equilibration buffer" and "pH of the equilibration buffer" on the response parameters "specific activity" and "recovery yield" of the total flowthrough and "purification factor" of single flowthrough fractions by a multivariate DoE screening approach. We assumed that the performance of the mixed mode resin, where adsorption and desorption happen due to hydrophobic interactions and ionic charges, is affected by the ionic strength and the pH value of the equilibration buffer. We also tested different flow rates, since it is commonly known that equilibrium between the stationary and the mobile phase can be adjusted more efficiently at low flow rates.

Before the different DoE experiments, we determined the column performance parameters of the manually packed bed. AF was determined with 1.24 $\pm$ 0.006 and N/m with 1,912 $\pm$ 160 m^{-1}. Both parameters were within the range recommended by the supplier (*i.e.* AF: 0.8 – 2.0; N/m: 1,000 – 3,000 m^{-1}). Adequate column packaging and performance was assured throughout the DoE experiments as column performance parameters did not significantly differ after the purification runs.

We performed 11 experiments suggested by the program MODDE (Table 3) with cell-free fermentation broth, determined the protein concentration and the catalytic activity in the crude extract, the flowthrough and the single eluted fractions and calculated the specific activities, the recovery yields and the purification factors. For all purification runs in this DoE study neither diafiltration nor post-load low-salt wash were conducted.

The multivariate approach revealed the flow rate to be a non-significant factor, as the calculated regression coefficient was smaller than the confidence intervals. However, as shown in Figure 13, the two factors ionic strength and pH of the equilibration buffer significantly affected the performance of the mixed mode resin.

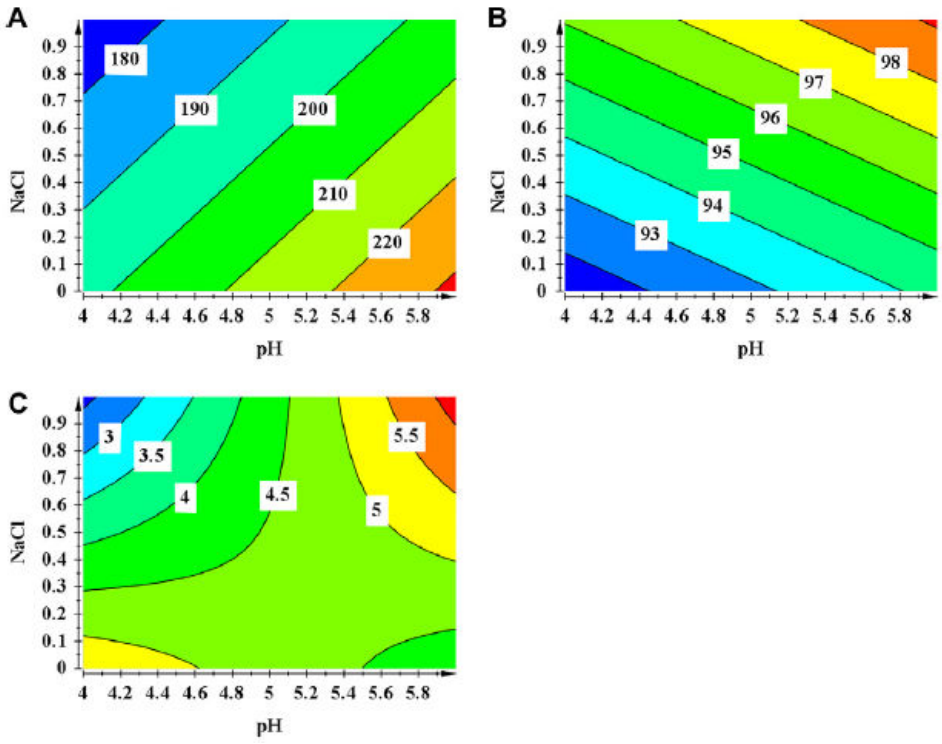

Figure 13: Response surface plot of the factors ionic strength and pH of the equilibration buffer in response to A) the specific activity of the total flowthrough, B) the recovery yield of the total flowthrough and C) the purification factors of single flowthrough fractions (fraction size 2 mL).

The specific activity of the total flowthrough (*i.e.* a pool of all flowthrough fractions) was higher, when less salt in the equilibration buffer was used (Figure 13A). However, a NaCl concentration of 1.0 M and a pH of 6.0 of the equilibration buffer gave a very high recovery yield of rHRP in the flowthrough (Figure 13B) and single flowthrough fractions with PFs of more than 6.0 (Figure 13C). Depending on the required purity and activity of the final enzyme preparation and the minimum recovery yield, the HCIC step can be adjusted according to Figure 13. Operating this step in flowthrough mode has several advantages over standard

purification techniques, such as the possibility to operate the system in a continuous mode, easy-to-perform scale-up, minimizing regeneration procedures of the resin and no need for elution buffers containing high salt concentrations and thus reduced cost and less harmful conditions.

SEC

Size-exclusion chromatography was applied for polishing partially purified rHRP. As mentioned above, screening experiments showed no apparent influence of the flow rate on the PF. However, to verify this observation and to further check if the sample volume might influence the purification performance, we varied the flow rate and the injected sample volume according to the experimental plan suggested by MODDE (Table 4). We chose these two factors, because it is commonly known that the flow rate and the sample volume can affect the resolution of SEC runs (e.g. [38]).

When we applied 0.5 mL sample and a flow rate of 35 cm/h we could not measure significant protein concentration or catalytic activity in any of the collected fractions, most probably due to dilution effects, and excluded this point from the multivariate analysis. For the other DoE runs, both factors “flow rate” and “sample volume” were determined as non-significant within the limits tested as the calculated regression coefficients were smaller than the corresponding confidence intervals. Purification factors of at least 2.0 were obtained in all SEC runs. Since the value for N/m did not change after the purifications, adequate column packaging and performance was assured.

In general, it is favourable to achieve high purity of the target enzyme and a maximum product yield in a reasonable time. Thus, both sample volume and flow rate have to be optimized to obtain an efficient SEC purification process. Here, it was possible to inject up to 5 mL sample, which corresponds to 4 % of 1 CV, and apply a flow rate of 35 cm/h and still obtain a PF of at least 2.0.

2.3.11 CIM monolithic columns

Monolithic columns have recently been discovered as powerful tool for both, analytical purposes and preparative protein purifications [39-41]. The solid support, a uniform monolithic porous material allows elevated operating flowrates and pressures, high binding capacities and is simple to handle and scale-up. These beneficial features are mainly enabled via convective mass transfer of the target molecules through the highly interconnected channel structure of the porous polymer block *e.g.* glycidyl mathacrylated based materials. On the other hand, porous particles applied in conventional chromatographic gel-media cause diffusive transport of the molecules, where they have to penetrate into the pores to get in contact with the active surface resulting in slow separation times and large void volumes. However, in convective interaction media both, resolution and binding capacity are not affected by the flowrate, an effect that is emphasized when large biomolecules such as proteins are separated due to their high diffusion coefficient [41].

A wide range of formats and ligands is available [42], however, the column-constructed phases investigated here were anion-exchangers and a hydrophobic interaction capsule. Different buffer systems, flowrates and elution profiles were tested for the potential application of CIM monolithic columns as a polishing step for rHRP expressed in *P.pastoris*. Flowthrough fractions from HCIC purifications were pooled and rebuffered and applied to the CIM-columns. The first principle tested was a CIM-OH colum, which is in fact a hydrophobic material and thus, was not able to purify rHRP after HCIC any further, because the vast majority of hydrophobic proteins was already retained on the mixed-mode resin. Thus, this principle was not suitable as a polishing step after HCIC.

The strong anion-exchanger CIM-QA could not purify the enzyme preparations more than 1.3-fold in initial experiments, which was also observed with particle-based anion-exchange materials before [17], probably due to the inacessability of the protein to the stationery phase

caused by the extended glycan structure preventing ionic interactions between protein and ligands. Hence, this principle was not investigated any further.

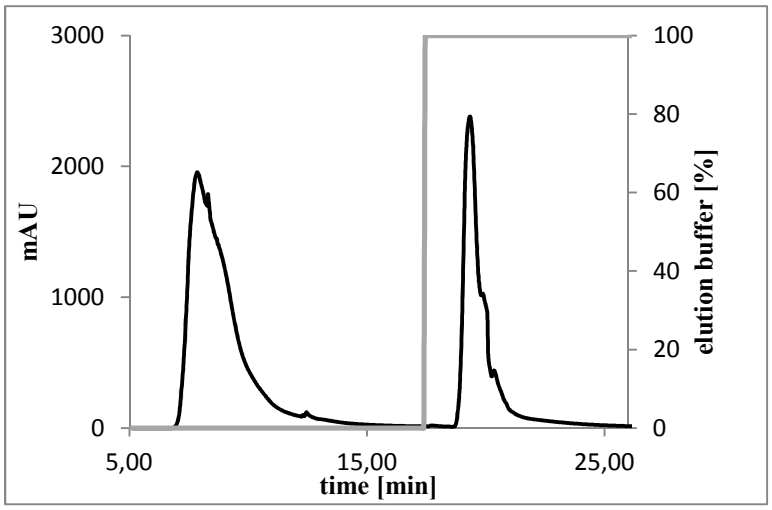

Figure 14: Chromatogram of a CIM-DEAE run with partially purified rHRP after HCIC. Instead of a gradient elution, a step-wise elution from 0 – 100 % elution buffer was performed. Black line, UV signal; grey line, concentration of elution buffer.

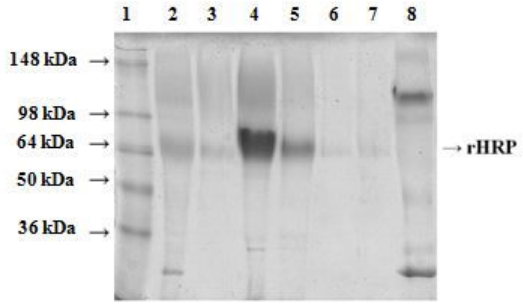

Figure 15: SDS-PAGE of fractions from CIM-DEAE of partially purified rHRP after HCIC . Lane 1, molecular mass standard (5 µg); lane 2, partially purified rHRP after HCIC (5 µg); lane 3-7, flowthrough fractions of CIM-DEAE (between 5 - 7 µg): lane 8, eluted fraction.

The second monolithic ion exchange colmn tested was a CIM-DEAE, a weak anion-exchanger. For binding, pH values between 6.0 and 8.0 were tested and loading was conducted at different flowrates. The target protein again did not bind to the column, but contaminating proteins bound to the monolithic surface and purification factors between 1.8 and 2.5 were achieved in flowthrough fractions (Figure 15, Figure 14, lanes 4-5). The most

successful buffer system for binding of impurities was a TrisCl-buffer at a pH of 8.0 and as the target protein was not retained on the stationery phase, a simple one-step elution was sufficient to regenerate the column (Figure 15; - lane 8). A summary of the univariate experiments with CIM-monolithic colums and their corresponding results is presented in Table 6.

Table 6: Summary of purification strategies using CIM-monolithic colums.

principle/resin	**operation mode**	**PF**	**recovered rHRP [%]**
CIM-DEAE 1 Monolithic column	flowthrough	≥ 2.0	80
CIM-QA 1 Monolithic column	flowthrough	1.2	70
CIM-OH 1 Monolithic column	flowthrough	1.5	30

2.4 Conclusions

We screened a variety of common protein purification techniques to develop a suitable strategy for the purification of hyperglycosylated rHRP produced in *P. pastoris*. More than 40 chromatography runs applying different resins, buffers and pH values were tested in a univariate manner. Promising strategies were subsequently analyzed in more detail in a multivariate DoE screening approach to identify factors significantly influencing the purification performance. Finally, we suggest a 2-step strategy comprising

1) a HCIC step with a MEP HyperCel resin operated in flowthrough mode. The cell-free fermentation broth can be applied directly and does not have to be diafiltrated with binding buffer. Since this step is operated in flowthrough-mode also the post-load low-salt wash can be spared shortening the overall process time. Equilibration of the resin with a buffer containing 1.0 M NaCl at pH 6.0 resulted in flowthrough fractions with a PF of more than 6.0.

2a) a SEC step with a Superdex 75 pg resin for polishing. A sample volume of up to 5.0 mL, corresponding to 0.04 CV, and a flow rate of 35 cm/h can be applied resulting in a PF of at least 2.0.

2b) According to the results from univariate experiments with CIM-monolithic colums, we suggest as a second step a CIM-DEAE purification using TrisCl pH 8.0 as binding buffer, which gave purification factors between 1.8 and 2.5. This system can be operated at higher flowrates and is easier to scale-up than traditional size exclusion chromatography. Moreover, the sample is not exposed to room temperature for a long timespan if the column is not cooled. This purification can be performed in a flow-through mode too, making it a superior method to slow size-exclusion chromatography. Furthermore, there is no need for complex elution profiles or high-salt concentrations, upgrading this method once more.

In both steps more than 85 % of the applied rHRP were recovered. A summary of this 2-step strategies is shown in Table 7 and Figures 16 and 17.

Table 7: Purification table describing the efficient 2-step strategy to purify hyperglycosylated rHRP produced in *P. pastoris*.

purification step	volume [mL]	total protein [mg]	total activity [U]	specific activity [U/mg]	purification factor	Yield [%]
crude extract	100	40	3,100	77	1	100
HCIC	20	~7	2,900	400	> 5	93
SEC	1	~3	2,900	1,000	≥ 2	100
CIM-DEAE	1	~3	2,900	1,000	≥ 2	75

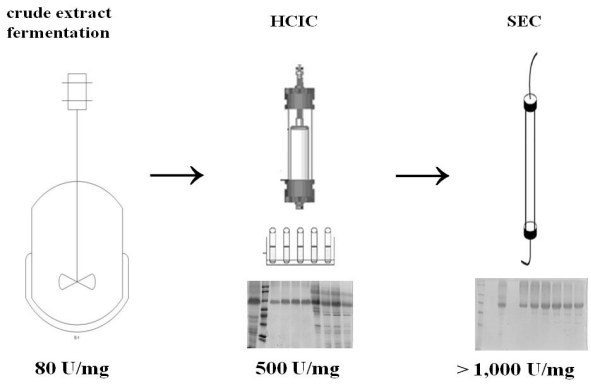

Figure 16: Graphic summary of a fast and efficient purification strategy for rHRP produced in *P. pastoris* applying HCIC and SEC.

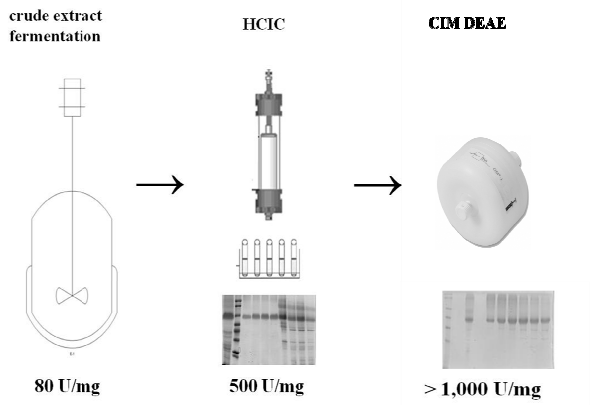

Figure 17: Graphic summary of a fast and efficient purification strategy for rHRP produced in *P. pastoris* applying HCIC and a monolithic column.

Compared to the commercially available, quite expensive HRP isolated from plant, of which the specific activity is given with around 1,000 U/mg by the supplier (Sigma-Aldrich, P6782-100MG), the here presented 2-step strategies for the purification of rHRP from *P. pastoris* can be regarded as competitive in terms of specific activity of the purified enzyme and describes a simple and fast purification strategy.

3 Glycoengineering of recombinant horseradish peroxidase expressed in *P. pastoris*

3.1 Introduction

The yeast *P. pastoris* has been successfully applied for the recombinant expression of fully active horseradish peroxidase [15, 16]. However, the extensive glycosylation of the recombinant enzyme from *P. pastoris* hampers an efficient purification process applying conventional chromatographic methods [17]. Moreover, when rHRP should be used *in vivo* for medical applications, *i.e.* targeted cancer treatment together with IAA [10], the surface glycans cause immunogenic responses and are rapidly cleared from the liver. An enzymatic deglycosylation is not possible due to the sugar structure of glycans in *P. Pastoris* [5]. This is why the second chapter of this thesis deals with the reduction of the glycosylation pattern in a molecular biology approach. Mutations within the amino acid structure of HRP have already shown to be beneficial for the enzyme's stability and activity in some studies, *e.g.* [6, 7].

In a PCR-based approach, the amino acid Asparagine at position 57 was changed to Aspartate, Glutamine and Serine. The most beneficial mutated enzyme variant was expressed in a bioreactor and characterized in detail in comparison with wild type rHRP from *P. pastoris*.

3.2 Materials and Methods

3.2.1 Nucleic Acid Analysis

Electrophoresis of nucleic acids was performed in a Power Pac apparatus on 0.8% Agarose Gels (BioRad) stained with SybrSafe® (Fermentas). Gels were visualized in a GelDoc Universal Hoog II Apparatus (BioRad) and evaluated using the ImageLab® Software. Nucleic acid concentrations were measured at 260 nm using a NanoDrop ND_{1000} spectrophotometer (NanoDrop Technologies, Thermo Scientific) which was previously blanked with water.

3.2.2 Preparation of frozen stocks

For storage, the correct clone was conserved on a LB Zeocin™ plate and a frozen stock was prepared by cultivation of one colony in 10 mL liquid LB-medium containing 75 ng/µL Zeocin™. Thereof, 1 mL cells was mixed with 0.5 mL 70% glycerol and immediately frozen in liquid nitrogen and stored at -80°C. For *P. pastoris* strains, 10 mL YPD Zeocin™ (100 ng/µL) were inoculated with one colony and grown overnight at 28°C, 230 rpm. Glycerol was added to a final concentration of 25% and immediately frozen in liquid nitrogen. These *P. pastoris* stocks were used as inoculum for fermentation experiments.

3.2.3 Plasmid propagation in *E. coli*

A recombinant *E. coli* strain TOP10F' containing the plasmid pPpT4 S (Figure 18) carrying the gene for HRP C1A (provided by Prof. Anton Glieder, Technical University Graz), which was codon-optimized for *P. pastoris* including the α-prepro signal sequence from *S. cerevisiae,* was grown in 4 mL liquid low-salt LB (50 ng/µL Zeocin™) overnight at 37°C, 220 rpm. The cells were pelleted at 5000 rpm for 10 min, the plasmid was isolated using the

Quiagen® MiniPrep-kit and a restriction analysis with *EcoRI* (Fermentas, Austria) was performed and analyzed on a 0.8% Agarose-gel.

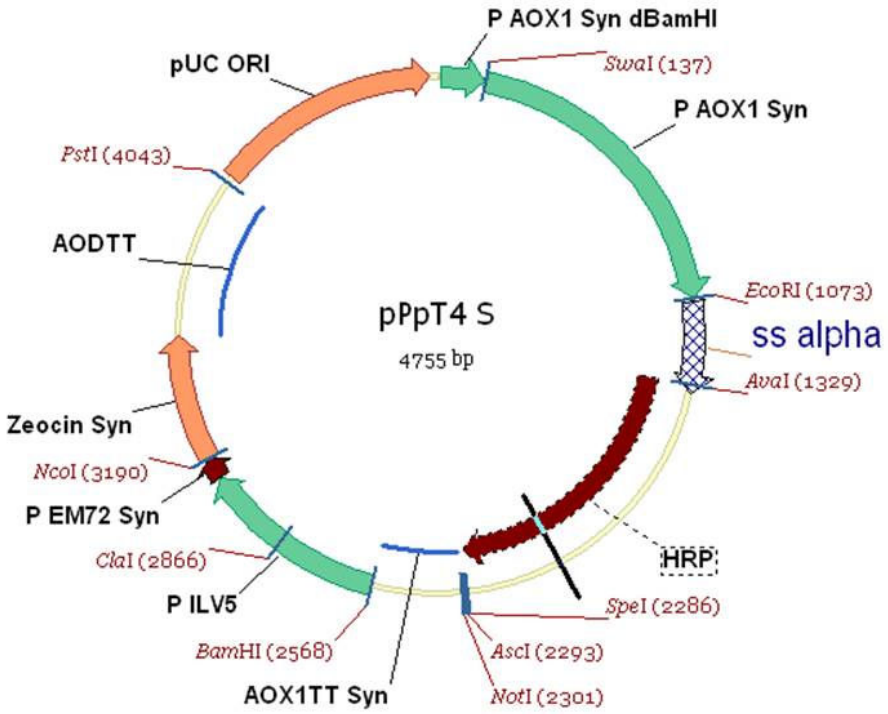

Figure 18: Shuttle vector containing the gene for HRP. The plasmid pPpT4 S (constructed at the Technical University of Graz) contains typical structural elements for a *P. pastoris* shuttle vector such as the AOX1 promoter (P AOX1 Syn) and terminator (AOX1TT Syn) elements, a *S. cerevisiae* secretion signal (SS alpha), the orignial HRP gene (codon-optimized for *P.pastoris*), a selectable marker (Zeocin^{TM}), an origin of replication (pUC ORI) for plasmid maintainance in *E. coli* and multiple cloning sites (e.g.*Not*I, *Swa*I, *Eco*RI).

3.2.4 PCR

To introduce the respective mutation (N57→Q/D/S), mutant primers (synthesized from LGC genomics) were designed in a Splicing by Overlap Extension (SoE) approach, whereby only the forward primer contained the desired mutation. The primers were designed with a 15 bp 5‘overhang from the amino acid to be substituted, the corresponding reverse primers did not contain the mutation (Figure 19 and Table 8).

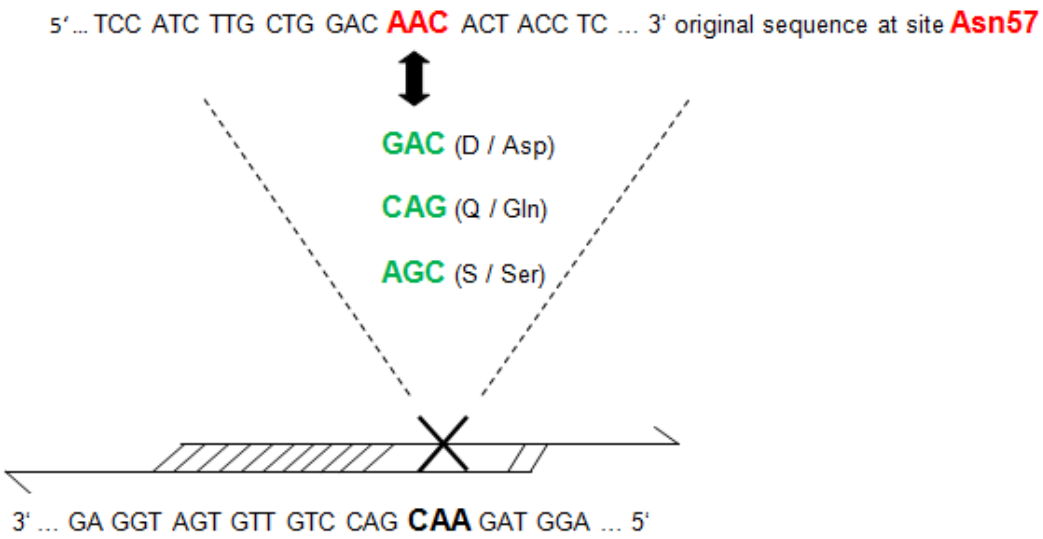

Figure 19: SoE primer design. To remove the *N*-glycosylation site N57 (Asn57, red), the codons for Asparagine (AAC) were changed to the corresponding triplets of the three structural similar amino acids Aspartate (GAC), Glutamine (CAG) and Serine (AGC) by designing mutant forward primers and the original-sequence reverse primer.

Standard PCR-reactions were carried out using Phusion® DNA Polymerase (Fisher Scientific, Vienna) in a S1000™ Thermal Cycler (BioRad). The wildtype plasmid pPpT4 S (Figure 18) was used as a template in amounts of 4.6 ng per reaction. Primers were added to a final concentration of 0.5 µM (Table 8), dNTPs of 10 mM.

Table 8: Primers for SoE PCR, site-directed mutagenesis.

Primer	Sequence	melting temp. [°C]
N57D fwd	TCC ATC TTG CTG GAC **GAC** ACT ACC TC	61,6
N57Q fwd	TCC ATC TTG CTG GAC **CAG** ACT ACC TC	61,4
N57S fwd	TCC ATC TTG CTG GAC **AGC** ACT ACC TC	61,9
N57X rev	GTC CAG CAA GAT GGA AGC ATC ACA ACC	61,7

Annealing temperature was chosen to be 2°C below primer's melting temperature and performed in a step gradient of 59-62-64°C. The elongation time (72°C) was calculated to be

150 sec (30 sec/kb), expecting a PCR product of approx. 5 kb. Three cycles of this programme were performed (Table 9). The product was digested for 1.5 h at 30°C with *Dpn*I to yield an unmethylated product for the plasmid ligation in *E. coli* TOP10F‘ (*vida infra*) and purified using a PCR clean-up kit (Quiagen®) and analyzed on an 0.8% Agarose gel before transformation.

Table 9: PCR programme for SoE.

Step	Temperature [°C]	Time [sec]
Initial denaturation	98	30
Denaturation	98	10
Annealing	59 / 62 / 64	30
Elongation	72	150
	72	10 min

3.2.5 Transformation of the mutated plasmids into *E. coli* TOP10F‘

A frozen stock of *E. coli* TOP10F‘ was propagated in 300 mL TB medium in a 1000 mL shake flask from a 4 mL overnight preculture (37°C, 220 rpm) until an OD_{600} value of approx. 0.6, pelleted for 15 Min. at 4000 x g, 4°C and resuspended several times in ice-cold 10 % glycerol and finally taken up in 1 mL glycerol to yield a concentration of 1-3 x 10^{10} cells/mL. Aliquots of 50 µl were immediately frozen in liquid nitrogen and stored at -80°C until further use. The transformation mixture consisted of 50 µl frozen *E. coli* TOP10F‘ (thawed on ice) and 5 µl of purified PCR product containing the HRP genes (average concentration of PCR products: 96 ng/µl). Electroporation was performed using a MicroPulser Electroporator (BioRad). Parameters were 1.5 – 2 kV for > 5 ms. Cells were immedeatly regenerated in 500 µl temperated TB medium and incubated for 1.5 h at 37°C h, 200 rpm and afterwards selected on LB-Agar plates containing 75 ng/µL Zeocin™. From each plate, 8 colonies were picked and grown at 37°C, 210 rpm in 5 mL low salt LB medium containing 100 ng/µL Zeocin™ in

15 mL sterile falcon tubes. Cells were harvested after 14 h by centrifugation and the plasmids were purified using the Quiagen® MiniPrep kit. Purified plasmids were analyzed on a 0.8% Agarose gel after linearization with *EcoRI* (37°C, 1 h) and prepared for sequencing with *AOX1*-specific flanking primers (Table 10). Approximately 1 µg of purified plasmid was mixed with the respective primer (100 µM primer per reaction mixture). Sequencing service was accessed from LGC Genomics (United Kingdom) or Microsynth GmbH (Switzerland).

Table 10: Flanking primers for sequence analysis.

Name	Sequence	Melting temp. [°C]
pAOX fwd	GCGACTGGTTCCAATTGACAAG	56.7
pAOX TT rev	CATCTCTCAGGCAAATGGCATTC	56.5

Correct transformants were cultured in 4 mL LB Zeocin^{TM} (100 ng/µl) for the propagation of the plasmid to obtain sufficient amounts for the transformation into *P. pastoris*. Plasmids were linearized with *SwaI* and purified using a PCR purification kit (Quiagen) and analyzed on a 0.8% Agarose gel.

3.2.6 Transformation into *P. pastoris* SMD1168H and CBS7435 & colony screening

A frozen stock (-80°C) of a *P. pastoris* strain SMD1168H (Invitrogen) or CBS7435 (provided by Prof. Anton Glieder, Graz University of Technology, Austria) was cultured on YPD-Agar plates and propagated in 50 mL liquid YPD medium at 28°C, 220 rpm overnight in a 500 mL shake flask. From this culture, 1 mL was transferred in 50 mL fresh YPD and finally grown in 150 mL YPD to an OD_{600} of 1.2. The cells were harvested by centrifuging at 500 x g for 5 Min. at 4°C, washed with 9 mL BEDS buffer and 1 mL DTT (1 M) and finally resuspended in 1 mL BEDS buffer. From these competent cells, 80 µl were used for electroporation. The amount of plasmids obtained from *E. coli* (*vide supra*) was 6.5 µg on

average. After electroporation, cells were regenerated for 1.5 h in 1 mL YPDS at 28°C, 150 rpm in 2 mL sterile Eppendorf tubes before selection on YPD(S) + Zeocin™ plates (100 ng/µl). After 3 days, 5 clones holding the HRP plasmids with different mutations (N57 → D/Q/S) were picked and analyzed for heterologous protein expression. As a negative control, an empty pPiCZ-alpha C vector (Invitrogen, Carlsbad; Figure 20) was propagated as described above and linearized with *SacI* and transformed in the same manner as the HRP plasmids.

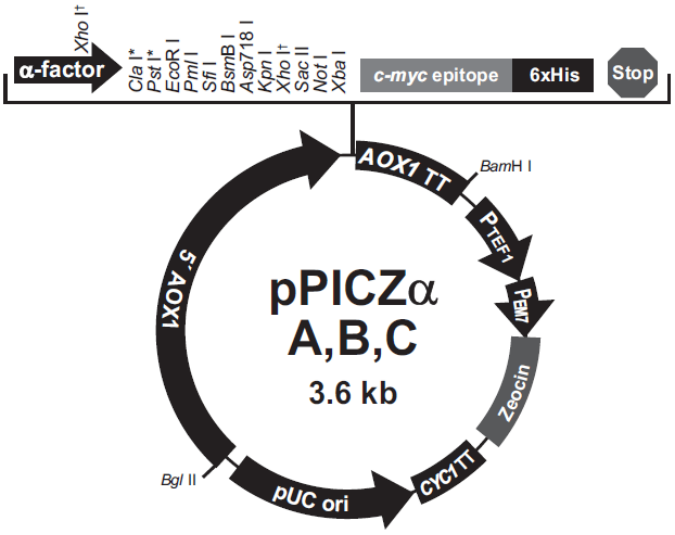

Figure 20: Shuttle vector pPICZα-series. The empty vector pPICZα-C was propagated in *E. coli* and linearized with *SacI* before transformation in to *P. pastoris* CBS7435 in order to confer Zeocin™-resistance, but not the HRP gene. This strain was used as background control to check for native *P. pastoris* proteins [43].

3.2.7 Expression of rHRP in *P. pastoris*

Five colonies of each clone (D/Q/S substituted mutant; wild type rHRP and the empty pPiCZα-C vector as controls) were picked with a sterile toothpick and grown in 15 mL BMGY in 100 mL shake flasks to a final OD_{600} of approx. 10. Appropriate volumes of the culture were resuspended in 25 mL BMMY to yield a starting OD_{600} of approximately 1 for the induction of heterologous protein expression. Samples were taken at least every 24 h and analyzed as described in "Analysis of expression". To balance methanol evaporation and

consumption, pure methanol was added to the culture to yield a final concentration of 1% (v/v) every 24 h. δ-Aminolevulinic acid (δ-Ala) or $FeSO_4$ was added, if necessary toa final concentration 1 mM from a 50 mM stock solution. Positive clones were confirmed by colony PCR (*vide infra*) and cultured in 150 mL medium containing 100 ng/µL Zeocin™ in 1 L baffled flasks (28°C, 210 rpm) to obtain sufficient amounts for biochemical characterization, stability tests and initial purification experiments.

3.2.8 Analysis of expression

Biomass was determined photometrically by measuring the absorbance at 600 nm (OD_{600}) in a Genesys VIS-Spectrophotometer (Thermo Scientific, Vienna). Dry cell weight of fermentation samples was determined gravimetrically by centrifuging 5 mL of fermentation broth for 10 Min. at 5000 rpm, 4°C washing the pellet with 5 mL deionized water before drying for 72 h at 100°C in a drying oven. Samples were centrifuged at 14 000 rpm, 10 Min, 4°C. From the supernatants, protein contents were determined at 595 nm by the Bradford assay using the BioRad Protein Assay Kit with bovine serum albumin (BSA) as standard in the range of 0.1 – 1.6 mg/mL. The enzymatic activity of HRP was determined using a CuBiAn XC photometric robot (OptoCell, Germany). Samples (10 µl) were added to 140 µl of 1 mM ABTS (2.2' azino bis 3-ethylbenzthiazoline-6-sulphonic acid) in 50 mM KH_2PO_4 buffer (pH 6.5).The mixture was incubated at 37°C and the reaction was started by the addition of 20 µl of 0.075% (v/v) H_2O_2. Changes of absorbance at 415 nm were measured for 80 seconds and rates were calculated automatically. Calibration was done with commercially available HRP (P8375, Sigma–Aldrich) at six different concentrations (0.02–2.0 U/mL). Samples were diluted either manually or automatically, if necessary. Methanol concentrations were measured by HPLC (Agilent Technologies, USA) equipped with a Supelcogel C-610 H ion-exchange column (Sigma-Aldrich, USA) and a refractive index detector (Agilent Technologies, USA). The mobile phase was 0.1% H_3PO_4 at a constant flow rate of 0.5

mL/min and the system was run isocratic. Calibration was done by measuring standard points in the range of 1 to 20 g/L methanol.

The *P. pastoris* strain SMD1168H was additionally analyzed for intracelluar protein content and activity. Therefore, biomass from 1 mL culture was resuspended in 300 µL Breaking Buffer and an equal volume of acid-washed glass beads (0.5 mm diameter; Sigma-Aldrich, Germany) was added, vortexed for 30 seconds and placed on ice for 30 seconds. This procedure was repeated for 8 cycles before separating the supernatant by centrifuging at 14 000 rpm for 10 Min.

Electrophoresis was done in a vertical Mini-Protean Tetra Cell apparatus (Biorad, Austria) at 150 – 200 V constant in 1 x Tris-Glycine buffer. Protein samples were loaded in amounts of 1-10 µg onto the gel, unless otherwise noted. The protein mass standard used was the Benchtop Prestained Ladder (Fermentas, Austria) in the range of 20 – 250 kDa. Gels were stained with standard Coomassie-stain and scanned with a conventional office scanner.

3.2.9 Colony PCR of expressing clones (*P. pastoris* CBS7435)

From the best expressing clones (one for each substitution, wild type HRP and empty vector pPiCZα-C as controls), a biomass sample was taken with a sterile toothpick and dissolved in 0.2% sodium-dodecylsuflate (SDS) and heated at 94°C for 4 minutes, centrifuged for 10 Min. at 14 000 rpm and the supernatant was used as a template for consecutive colony PCR with Phusion® HF polymerase and *AOX1*-specific primers (Table 11).

Table 11: AOX1-specific primers for sequencing and colony PCR of P. pastoris CBS7435.

Primer	Sequence	melting temp. [°C]
pAOX1_fwd cPCR	5'-GCG ACT GGT TCC AAT TGA CAA-3'	55.8
AOX TT_rev cPCR	5'-CAT CTC TCA GGC AAA TGG CAT T-3'	55.6

A detailed description of the colony PCR programme is shown in Table 12. The result was analyzed by Agarose-Gel electrophoresis. To confirm the correct mutation within the HRP gene, the corresponding PCR product (1.4 kB) was excised from the Agarose gel an purified using the GelExtraction Kit (Quiagen®) and sequenced (Mircosynth GmbH, Switzerland).

Table 12: PCR programme for colony PCR using AOX1-specific primers.

	Temperature [°C]	Time [sec]
Initial denaturation	98	30
Denaturation	98	5
Annealing	56.6	10
Elongation	72	72
Final extension	72	10 min

3.2.10 Temperature stability

The supernatant of large-scale shake flask expression was harvested, concentrated and rebuffered in 50 mM potassium phosphate buffer, pH 6.5 using crossflow-filtration (Pall Centramate 500 TFF) and 10 kDa cutoff centrifugal filter units (Millipore, UK). Concentrated and rebuffered supernatants were diluted to approximately 1.5 U/mL in 50 mM Potassium-Phosphate buffer, pH 6.5 and incubated on a thermoblock at 50°C.

Samples of 200 µL were taken at a given timepoint, incubated on ice and precipitates were removed by centrifugation at 14 000 rpm for 5 Min, 4°C. Residual catalytic activity was measured photometrically with the substrate ABTS using the CuBiAn^{XC} photometric robot as described above. Inactivation constants were derived from a semi-logarithmic plot of residual activity over time and inactivation constants were calculated according to Equation 8 and rHRP vaiants were compared to the wild-type enzyme as well as to plant HRP (Sigma-Aldrich).

$$\tau_{1/2} = -\frac{k}{60}[Min] \quad \text{(Equation 8)}$$

, where $\tau_{1/2}$ is the half-life time in Min and k the inactivation constant, which was derived from the negative slope of the inactivation plot.

3.2.11 Bioreactor cultivation

Bioreactor setup

Fermentation experiments were performed in a 2.5 L working volume glass fermenter with a double-wall jacket for temperature control (Infors, Switzerland), which was measured by a temperature sensor (Infors, Bottmingen). Dissolved oxygen (dO_2) was measured with a polarographic dO_2 electrode (Hamilton, Switzerland) and pH using a sterilizable electrode (Hamilton, Switzerland) and maintained at 5.0 using ammonia solution (3.5 – 4 M) throughout the whole experiment. Base consumption and reactor weight was determined gravimetrically. Biomass estimation for the control of feeding-rates was calculated using an in house-developed Kalman-filter. Off-gas was measured with an infrared cell for CO_2 and a paramagnetic cell for O_2 and logged in a process information management system (PIMS, Lucullus, Biospectra, Switzerland). Air and oxygen inlets were equipped with sterile air filters and flowrates were regulated by mass flow controllers. Feeds and base were forwarded using peristaltic pumps.

Batch fermentations

As a pre-culture, 0.5 mL of a frozen stock (-80°C) of the corresponding *P. pastoris* CBS7435 strain (wild type rHRP, rHRP_N57S) was inoculated in YNBM (100 ng/µL Zeocin^{TM}) and cultured at 30°C, 230 rpm for 27 h in a 1000 mL shaking flask in a temperature controlled shaking incubator. From this preculture, 75 mL were transferred aseptically to the bioreactor

as inoculum for 1 L batch medium. BSM was previously sterilized directly in the reactor and pH was adjusted with NH_4OH to 5.0 after autoclaving. Trace element solution was added directly to the fermenter aseptically. The culture was cultivated at 30°C during batch fermentation, agitation was set to 1495 rpm and dO_2 was kept above 30% for the whole experiment and aerated with 1.25 vvm dried air.

Fed-batch fermentations

Temperature was set to 28°C, the culture was aerated with 1.25 vvm dried air and supplemented with pure oxygen, if necessary to keep dO_2 levels above 30%. After the glycerol batch phase, a glycerol fed-batch was started to generate sufficient biomass for subsequent induction. After complete depletion of the substrate glycerol from the fed-batch phase, the culture was adapted to methanol consumption by pulsing 0.5 % (v/v) methanol including trace element solution PTM1 and the ferric supplements δ -Ala and $FeSO_4$ was added at the timepoint of induction. Both, glycerol and methanol fed-batches were regulated by an in-house developed Kalman-Filter which controlled forwarding the substrate by a peristaltic pump to maintain a given specific growthrate (μ). Adapting μ to a desired specific substrate uptake rate (q_S) of 2 mmol g^{-1} h^{-1} for glycerol and 1 mmol g^{-1} h^{-1} for methanol, respectively and a biomass to substrate yield ($Y_{X/S}$) of 0.45 g/g for glycerol and 0.3 g/g for methanol, specific growth rates were calculated as 0.1 h^{-1} for glycerol growth and 0.01 h^{-1} for the induction phase when using methanol as sole carbon source. Samples were analyzed as described in "Analysis of expression".

3.2.12 Processing the fermentation broth and purification applying HCIC and CIM-DEAE

The fermentation broth was harvested and microfiltrated over a 0.2 μM membrane using the TFF system Centramate 500S (PALL) with a total filtration area of 0.3 m² at a max. flowrate

of 2.4 L/min. and a max. pressure of 1 bar not to harm the enzyme. For the glycoengineered enzyme variant, a additional centrifugation step (5000 rpm, 35 Min., 4°C) was performed before microfiltration. Subsequently, the clarified enzyme solution was concentrated using a 10 kDa cutoff membrane (Omega T-series; PALL, Austria) and rebuffered in 50 mM potassium phosphate, 1 M NaCl pH 6.0 for subsequent chromatographic purification using the mixed-mode resin MEP HyperCel (PALL) which was equilibrated in the same buffer. Loading flowrate was 1 mL/min before a step elution of 100% elution buffer and 0.5 M NaOH for 30 Min. was performed. This purification strategy is described elsewhere in more detail (Chapter I, [17]). Fractions were analyzed for protein content and catalytic activity and visualized on SDS-PAGE applying the same methods as described in "Analyisis of expression".

Purified flowthrough fractions of HCIC purifications were pooled and rebuffered in 50 mM KH_2PO_4 and approximately 43 mg protein solution (wild-type HRP) or 14 mg (rHRP N57S) were loaded onto a CIM-DEAE monolithic column at a flowrate of 1 mL/min. After washing with approximately 4 CV of binding buffer, a one-step elution of 100% elution buffer was performed, before regeneration with 0.5 M NaOH and restoring the column with 0.2 M MOPS buffer, pH 6.5 (+/- 1 M NaCl). Flowthrough and eluted fractions were analyzed as described in "Analysis of expression".

3.2.13 Characterization of rHRP variants

K_M and k_{cat} values of purified enzyme variants

After purification, the enzyme solutions were concentrated using 10 kDa cutoff centrifugal filter units and sterile filtered over a 0.2 µM filter. All reactions were carried out at 30°C in a total reaction volume of 1 mL whereby H_2O_2 concentrations were constantly 1 mM in all

reactions as a saturating substrate. ABTS concentrations were varied from 0.05 – 10 mM. For dilution, ultra purified water was used. All components despite H_2O_2 were mixed in cuvettes and placed into the thermostated spectrometer. Reactions were started by adding the respective amount of H_2O_2 and changes of absorption (mAU) at 420 nm at different substrate concentrations were recorded for 1 min. using a UV/Vis-Spectrometer (Hitachi) and ΔmAU was calculated. Protein concentrations of the enzyme solutions were 0.811 mg/mL for wild-type rHRP and 0.699 mg/mL for the N57S variant as determined by the Bradford Assay. At a given substrate concentration, the volumetric and specific activity was calculated and a Michaelis-Menten plot was diagrammed using the SigmaPlot Software and K_M and v_{max} were automatically computed. K_{cat} for ABTS was calculated using the following equation, approximating a molecular weight (MW) of 65 kDa (glycosylated) or 34 kDa (unglycosylated) for both enzyme variants and a timespan (t) of 60 sec.

$$kcat\_ABTS\ [sec^{-1}] = \frac{vmax\ [\mu mol * min^{-1}] * MW\ [kDa]}{\mathrm{t}\ [sec]} \qquad \text{(Equation 9)}$$

pH stability

The purified and concentrated enzyme preparations were incubated in different buffer systems in a temperature-controlled waterbath at 30°C for 30 min, incubated on ice and centrifuged at 14 000 rpm, 4°C for 15 min. to remove precipitates. From the supernatant, the residual catalytic activity was measured as described in “Analysis of expression” .

Glycosylation analysis

Purified rHRP samples were buffered in 0.1 M NH_4HCO_3 and reduced with DTT (5 mM) for 45 min at 56°C and alkylated using Iodoacetamide (25 mM) at room temperature for 30 min. The protein was precipitated with four volumes of acetone for 45 min at -20°C, dried in a

vacuum centrifuge and resuspended in 0.1 M NH_4HCO_3 buffer to yield a protein concentration of approx. 1 µg/µL. Digests were performed overnight with either Chymotrypsin or Trypsin (Promega) at 37°C at an enzyme-to-substrate ratio of 1:50 (w/w). The digested peptides were analyzed on a LC-ESI-MS system as follows: samples were loaded in amounts of 1-2 µg on a BioBasic-18 column (150 x 0.32 mm / 5 µm; Thermo Scientific) and eluted in a 0.3 % formic acid buffered (pH 3.0) acetonitrile gradient in a complex step-profile from 1 to 80 %. The LC system was an UltiMate 300 (Dionex, Thermo Scientific) operated at a flowrate of 6 µL/min, thus the separation took 60 minutes. Eluted peptides were analyzed on an Ultima Global Q-TOF mass spectrometer (Waters) operated in positive-ion mode, which was previously calibrated with a Caesium iodide standard in the range of 400 – 1800 *m/z*. Additionally, the peptide harbouring the site N57S within the mutated rHRP variant was fragmented in a MS/MS approach by selecting the ion mass 770.35 to be fragmented by collision induced dissociation (CID) applying Argon as collision gas. Data was manually evaluated and deconvoluted using the Software MassLynx V4.00.00 (Micromass Ltd, Manchester) whereby theoretical peptide masses were calculated by the ExPaSy-tool "Peptide Mass" using the settings: Iodacetamid, chymotryptic / tryptic, $[M+H]^+$. Interpretation of MS/MS spectra was aided by the web tool "Fragment Ion Calculator" (http://db.systemsbiology.net/proteomicsToolkit/FragIonServlet.html).

An aliquot of the chymotryptic digest was additionally treated with PNGase A to release the whole N-glycan structure from the amino-acid backbone. Prior to PNGase A digest, Chymotrypsin was inactivated by incubating the solution for five minutes at 100°C in a drying oven. Peptides were dried in a vacuum centrifuge and resuspended in a 50 mM citrate buffer pH 5.5 before adding PNGase A (1:1, w/v). After glycan release, peptides were removed by applying the peptide-glycan mixture to a centriufge-format porous graphite carbon column (Thermo Scientific), which was conditioned with both, ammonium-formiate buffer pH 3.0 and 50% acetonitrile before equilibration with five volumes of the aqueous

buffer. Subsequently, the protein-peptide solution was loaded onto the conditioned column and washed with formiate buffer before eluting the glycans in 50% acetonitrile, whereby peptides remained bound to the column. Glycans were analyzed using a Hypercarb column (100 x 0.32 mm / 5 µm, Thermo Scientific) in a combined stepwise-linear gradient from 1 to 50% acetonitrile on the same instruments applied for peptide analysis (*vide supra*).

3.3 Results and Discussion

3.3.1 Mutagenesis of HRP C1A and cloning of pPpT4 S_mut into *E. coli* TOP10F‘

The plasmid pPpT4 S carrying the original sequence for HRP was used as a template for site-directed mutagenesis of the glycosylation site N57 by SoE PCR using a mutant forward primer with a 15 bp overhang, homologous to the original reverse primer (Figure 19). The amino acid Asparagine was substituted with structural similar amino-acids (*i.e.* Glutamin, Serine and Aspartat) by changing the codon AAC to the corresponding triplet. The PCR products were demethylated by *DpnI*, successfully transformed into *E. coli* and transformants were selected on Zeocin™-containing plates, representing the colonies which have taken up the foreign DNA. On average, approximately 10 colonies resisted the selective pressure and were analyzed for their correct integration of the corresponding mutation by Agarose gel electrophoresis after a restriction analysis using *EcoRI,* which linearizes the plasmid pPpT4 S resulting in a fragment of 4.8 kB (Figure 21).

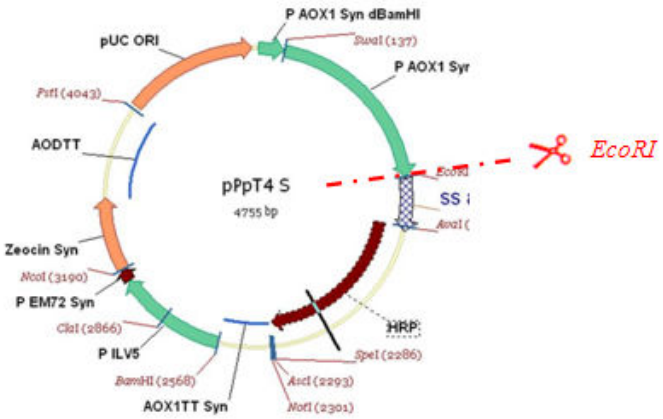

Figure 21: Restriction site of HRP-containing plasmid pPpT4 S using *EcoRI* for restriction analysis of *E. coli* transformants.

DNA was purified from the Agarose gel (Figure 22) and sequenced randomnly, unitl a correct transformant was identified. On average, every second clone contained the plasmid and

integrated the correct mutation. Colonies that did not contain the mutation according to sequencing have taken up the antibiotics resistance, but did not integrate the mutated HRP gene correctly. Sequences obtained from LGC genomics can be found as attachment.

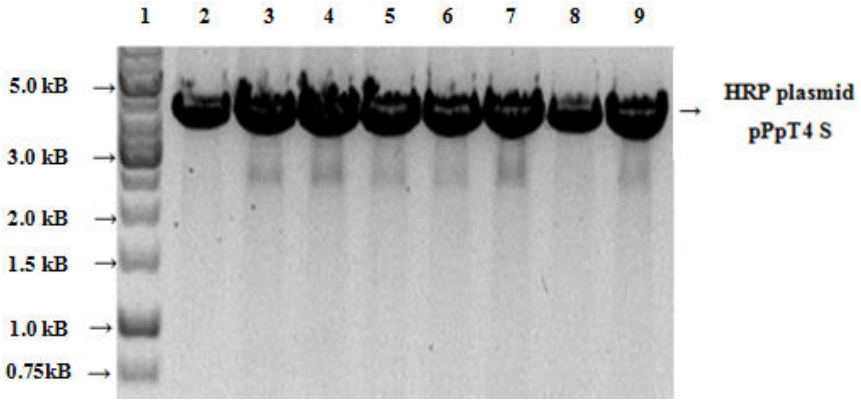

Figure 22: Restriction analysis of HRP plasmids propagated in *E. coli* . Lane 1, DNA-ladder; lanes 2-9, *EcoRI* restricted plasmids containing the gene for HRP (wild-type and D/Q/S substituted sequences).

3.3.2 Transformation into *P. pastoris* and expression screenings

Mutant plasmids were linearized and transformed into the protease-deficient *P. pastoris* strain SMD1168H and grown on glycerol before induction with a methanolic medium. After 72 h of induction, HRP activity was determined for the Serine-substituted mutant, but the amount of active enzyme was quite low (1.6 U/mL) and started to decrease five days after induction. Glutamin- and Aspartat-substituted mutants produced three days in delay, indicating problems with heterologous protein production of these enzyme variants. Wild type rHRP was also expressed in delay and HRP activity was not as high as it was observed before in other *P. pastoris* strains [16, 33].

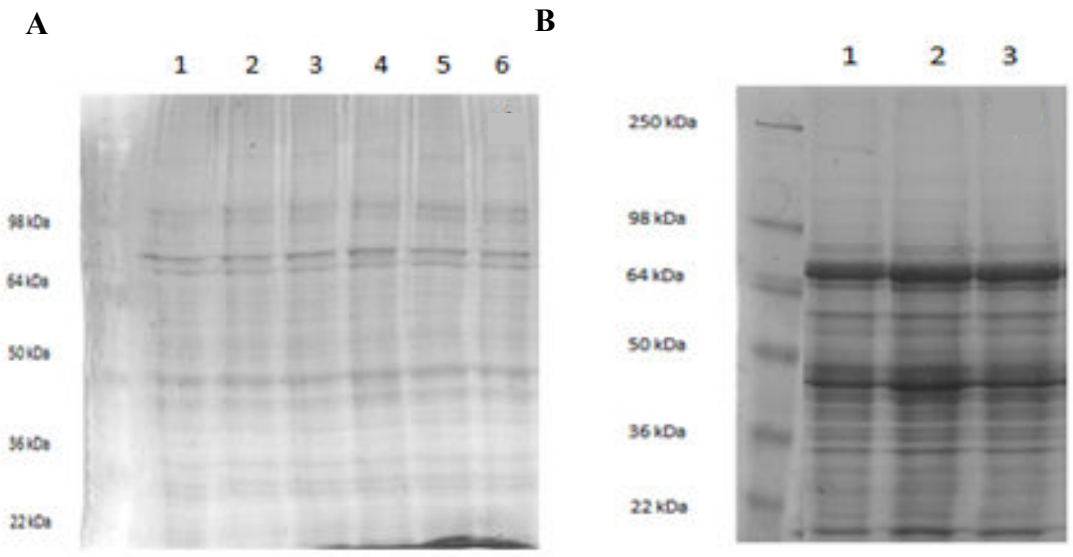

Figure 23: SDS-PAGE analysis of HRP expression in *P. pastoris* SMD1168H. A. extracellular space; left: molecular weight marker; lanes 1-6: different supernatants of SMD1168H_HRP_N57D/Q/S/wild-type. **B.** intracellular space; left: molecular weight marker; lanes 1-3: intracellular cell extracts from SMD1168H_HRP_N57D/Q/S. protein loads: 10 µg per lane.

According to SDS-PAGE (Figure 23A) rHRP was not significantly overexpressed extracellularly but in the intracellular space, a distinct band at 66 kDa is visibile (Figure 23B). When the intracellular space was analyzed, approximately 0.3 U/mL catalytic activity was detected in all clones. Thus, it is assumed that this strain had problems in processing the signal sequence and hence, was not able to secrete the heterologous protein but accumulated the target protein in the intracellular space.

Another explanation is that the gene of interest was not correctly integrated, *i.e.* incorrect homologous recombination at the *AOX1*-locus, as the plasmid was designed for another *P. pastoris* strain. Hence, this strain was not further investigated for HRP expression.

The plasmid-compatible strain *P. pastoris* CBS7435 was transformed and screened in the same manner as the SMD1168H strain. Enzyme activity was detectable starting from the second day after induction, and mutants showed up to 3-fold increased activity compared to

the wildtype enzyme. Again, the Serine-substituted mutant produced earlier and more active HRP, as previously observed in SMD1168H. A summary of expression analysis is shown in Table 13.

Table 13: Analysis of expression of rHRP in *P. pastoris* CBS7435.

***P. pastoris* clone CBS7435_HRP**	**protein content [mg/mL]**	**catalytic activity [U/mL]**	**specific activity [U/mg]**
N57D1	0.012	3.1	261.0
N57D2	0.107	0.962	9.0
N57D3	0.110	1.1	9.9
N57D4	0.109	0	0
N57D5	0	0	0
N57Q1	0.118	0	0
N57Q2	0.092	1.9	20.7
N57Q3	0.175	3.0	17.4
N57Q4	0.049	7.9	163.3
N57Q5	0.103	7.8	75.7
N57S2	0.104	7.9	76.3
N57S3	0.135	10.1	74.4
N57S4	0.072	1.9.	26.3
N57S5	0.162	8.0	49.5
wild type	0.066	3.2	48.5

As shown in Table 13, there were notable deviations in HRP productivity of the clones within the same amino acid substitution. This may result from multiple copy integration of the HRP gene as it is commonly observed in *P. pastoris* or from mis-integration of the target gene *i.e.* gene conversion events in which only parts of the vector has integrated at the *AOX1*-locus [20]. Thus, it is important to screen a statistically reasonable number of colonies in order to obtain an expressing clone. However, the clone with the best performance in terms of activity was chosen for upscaling and further analysis.

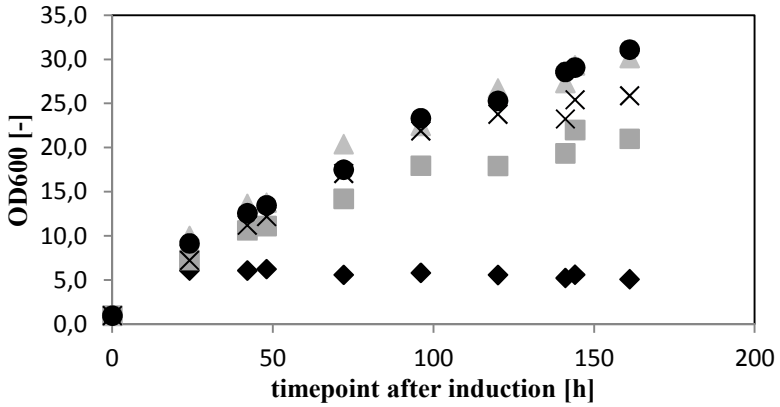

Figure 24: Methanol growth of *P. pastoris* CBS7435_HRP in shake flask experiments. OD600 over time. ◆ HRP_N57D ■ HRP_N57S ● HRP_N57Q ▲ wild type HRP HRP ×empty vector.

The respective *P.pastoris* strains were expressed in a larger scale and analyzed for protein content and activity. Interestingly, the *P. pastoris* strain containing Aspartat-substituted rHRP (N57D) had problems with growth on methanol as depicted in Figure 24. The OD remained stable at a value of approx. 6, whereby the other strains grew quite well and in a similar manner. When the same culture was inoculated in glycerol medium, no difference in terms of growth within the strains was observed (data not shown). This leads to the conclusion, that the reduced growth on methanol is not a physiological issue of the host strain, but a problem caused by this specific enzyme variant itself. An explanation thatfore is incorrect folding initiated by the Aspartate residue and thus, accumulation in the peroxisome resulting in a metabolic collapse of the cell. However, positive clones were analyzed using colony PCR and the integration of the correct mutation was confirmed by sequencing.

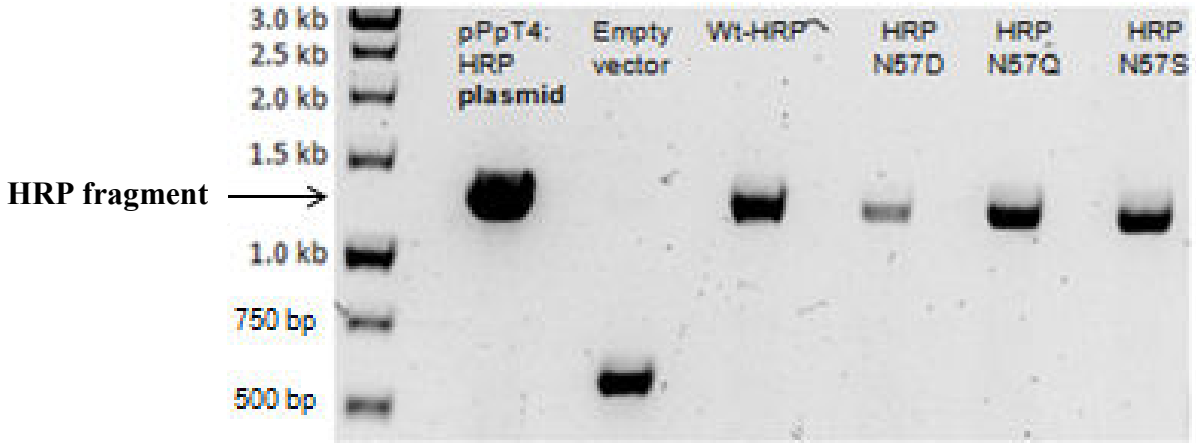

Figure 25: Agarose-gel analysis of colony PCR. Genomic DNA extracts were used as a template and analyzed on a 0.8% Agarose gel. Fragments were correctly sequenced.

As depicted in Figure 25, colony PCR from genomic extracts of the corresponding *P. pastoris* clones yielded a fragment at the predicted size, according to the primer binding sites at the *AOX1* promoter, transcribing the signal sequence and the HRP gene and stopping at the *AOX* terminator sequence. As expected, the PCR products showed a distinct band at 1.4 kb (Figure 25). As a positive control, the circular plasmid was used as a template. The empty vector was also transformed into the same CBS7435 strain and had undergone the same procedures as the HRP-containing mutants. A genomic DNA-extract thatof was used as a negative control and conferred Zeocine™ resistance to the native *P. pastoris* strain. However, the DNA fragments were purified from the agarose-gel and succesfully sequenced for their correct integration of the corresponding mutation (detailed sequencing data can be found as attachment). Surprisingly, colony PCR using conventional *Taq*-Polymerase was not successful due to the presence of many contaminating proteins and RNA from cell lysis. Neither a DNA extraction using a laborious procedure with organic solvents nor different PCR protocols (temperature gradients, varying primer concentrations etc) was successful when *Taq*-Polymerase was used. When the more expensive Phusion®-Polymerase was used, a simple lysis step using 0.2% SDS and the removal of cell debris by centrifugation was sufficient to yield a distinct PCR

product. Thus, when colony PCR from yeast cells is performed, one should use the freshest cells available and apply Phusion®-Polymerase instead of *Taq*.

3.3.3 Temperature stability

Glycosylation can influence thermostability of *P.pastoris*-derived proteins significantly [18]. Some studies reported increased thermostability of glycosylated proteins over non-glycosylated species, other researchers observed destabilizing effects [18, 44]. Hence, whenever the glycosylation process is altered, thermostability experiments should be performed because influences of glycans on the thermostability is strongly dependent on the individual protein.

For glycoengineered rHRP produced in *P. pastoris*, the best clone of each amino acid substitution was expressed in a larger scale in baffled shake flasks in order to obtain sufficient enzyme amounts for characterization and thermostability experiments. The rebuffered supernatants were incubated at 50°C and residual activity was measured photometrically. A semi-logarithmic plot was generated and inactivation constants and half-life times were calculated.

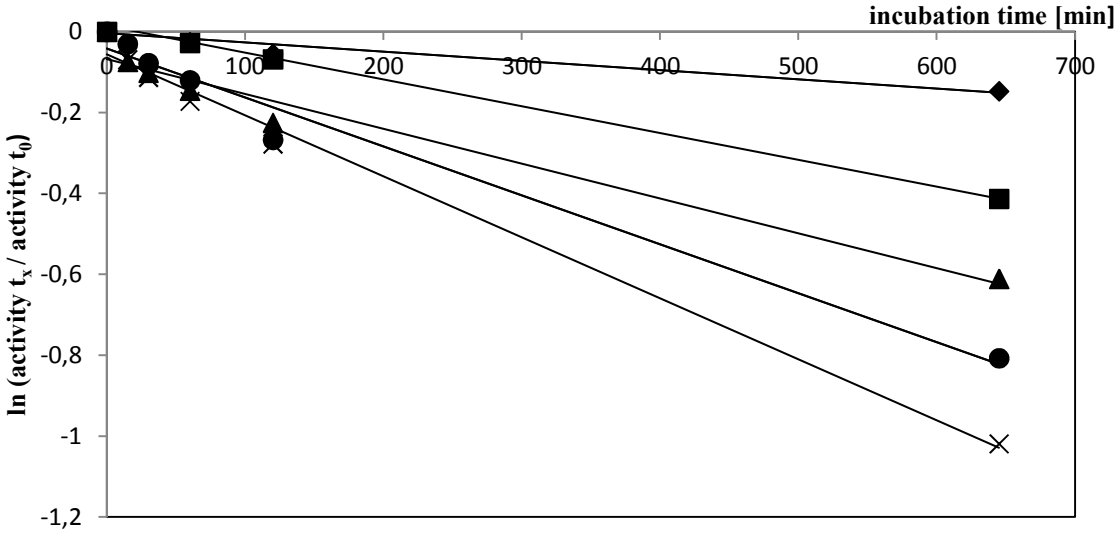

Figure 26: Temperature stabilities of HRP variants at 50°C. ◆ HRP_N57D ■ HRP_N57Q ▲ HRP_N57S ● HRP from *A.rusticana* × wild type HRP. Logarithmic values of the residual activity after incubation at 50°C were plotted over time and inactivation constants and half-life times were calculated.

Table 14: Inactivation constants and half-life times of HRP variants at 50°C. Inactivation constants were calculated from the negative slope of a semi-logarithmic plot (Figure 26) from residual activities over time and the corresponding half-life times were derived.

enzyme variant	inactivation constant	$\tau_{1/2}$ [h]
plant HRP	$1{,}2 \times 10^{-3}$	9,6
wt-HRP	$1{,}5 \times 10^{-3}$	7,7
N57D	2×10^{-4}	57,8
N57Q	7×10^{-4}	16,5
N57S	9×10^{-4}	12,8

As visible in Table 14 and Figure 26, all mutated HRP variants showed a higher thermal stability at 50°C as the wild type variant and the enzyme preparation from the horseradish root (Sigma). Interestingly, the Aspartate substituted mutant had an extraordinary high thermal stability compared to the other enzyme preparations. However, this was also the enzyme which caused problems in methanol growth in the host strain. The removal of the

glycans at a single site increased the thermostability of rHRP, but apparently also the amino acid substitution had an influence on the stability of the recombinant enzyme.

3.3.4 Bioreactor cultivations of *P. pastoris* CBS7435 expressing different HRP variants

Based on the the elevated activity values in shake-flask experiments and the increased temperature stability of the Serine-substituted mutant (HRP_N57S), this clone was chosen to be compared with the recombinant wild type enzyme. In order to obtain sufficient amounts of both rHRP variants (wild type and HRP_N57S) for subsequent characterization, fed-batch fermentations of the host strain *P. pastoris* CBS7435 were done. Heterologous protein expression of *P. pastoris* -derived proteins is strongly dependent on the cultivation conditions such as aeration, temperature or pH [18]. Thus, both cultivations were performed within exactly the same parameters in order to exclude different enzyme properties to be a cultivation artefact. Therefore, both rHRP variants were cultivated in a 2.5 L glass fermenter. A glycerol fed-batch for biomass generation was performed yielding a concentration of approximately 130 g/L biomass, followed by induction with a methanol-feed designed to maintain constant specific substrate uptake rate (q_S). Off-line samples were taken to confirm computed values and to monitor enzymatic activity and methanol consumption. Figure 27 represents the course of the carbondioxide evolution rate (CER) of both fermentations. The focus of these fermentations was not on the bioprocess itself but on maintaining a controlled environment for the production of comparable enzyme preparations.

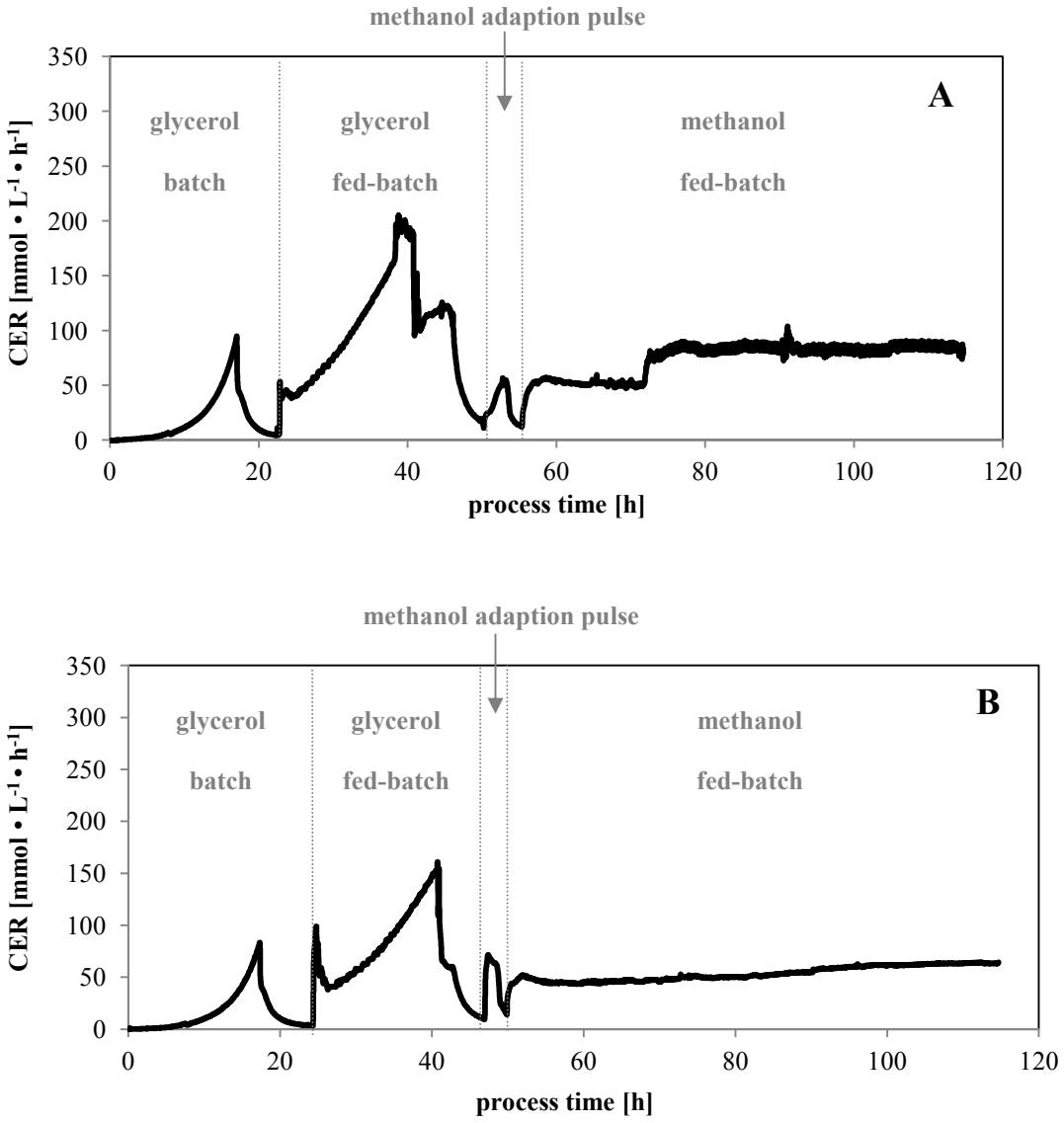

Figure 27: Fermentation of *P.pastoris*. Carbon dioxide evolution rate (CER). A, CER of strain CBS7435 expressing HRP_N57S; **B,** CER of strain CBS7435 expressing wild type HRP C1A. After biomass accumulation using glycerol as carbon source, HRP expression was induced with methanol.

Biomass was generated in a batch and a fed-batch phase using glycerol as carbon source. After depletion of the repressing substrate, a methanol adaption pulse (0.5% v/v) was performed to adapt the cells to the methanolic medium before a methanol fed-batch was started to maintain induction of heterologous protein expression. The adaption time Δt_{adapt} was determined from the timepoint of pulsing methanol to the point where a maximum of CER is

reached. For the strain expressing wild-type HRP, this value was approx. 1.2 h and 2.5 h for the glycoengineered HRP variant N57S.

Table 15: Bioreactor cultivation of *P. pastoris* CBS7435 expressing two different HRP variants. Specific growth rates for glycerol and methanol growth phases.

P. pastoris strain	average μ (glycerol) [h^{-1}]	average μ (methanol) [h^{-1}]
CBS7435_wild type HRP	0.039 ± 0.004	0.007 ± 0.003
CBS7435_HRP_N57S	0.044 ± 0.001	0.005 ± 0.002

Both, glycerol and methanol fed-batches were regulated by an in-house developed Kalman-Filter which controlled forwarding the substrate by a peristaltic pump to maintain a given specific growthrate (μ). Adapting μ to a desired specific substrate uptake rate (q_S) of 2 mmol g^{-1} h^{-1} for glycerol and 1 mmol g^{-1} h^{-1} for methanol, respectively and a biomass to substrate yield ($Y_{X/S}$) of 0.45 g/g for glycerol and 0.3 g/g for methanol, specific growth rates were calculated as 0.1 h^{-1} for glycerol growth and 0.01 h^{-1} for the induction phase when using methanol as sole carbon source. As visible in Table 15, both specific growth rates reached roughly the desired settings and thus, the Kalman filter has proven useful for the application in *P. pastoris* fermentations offering the advantage of running automated fed-batch experiments instead of manual control of the feeding regime.

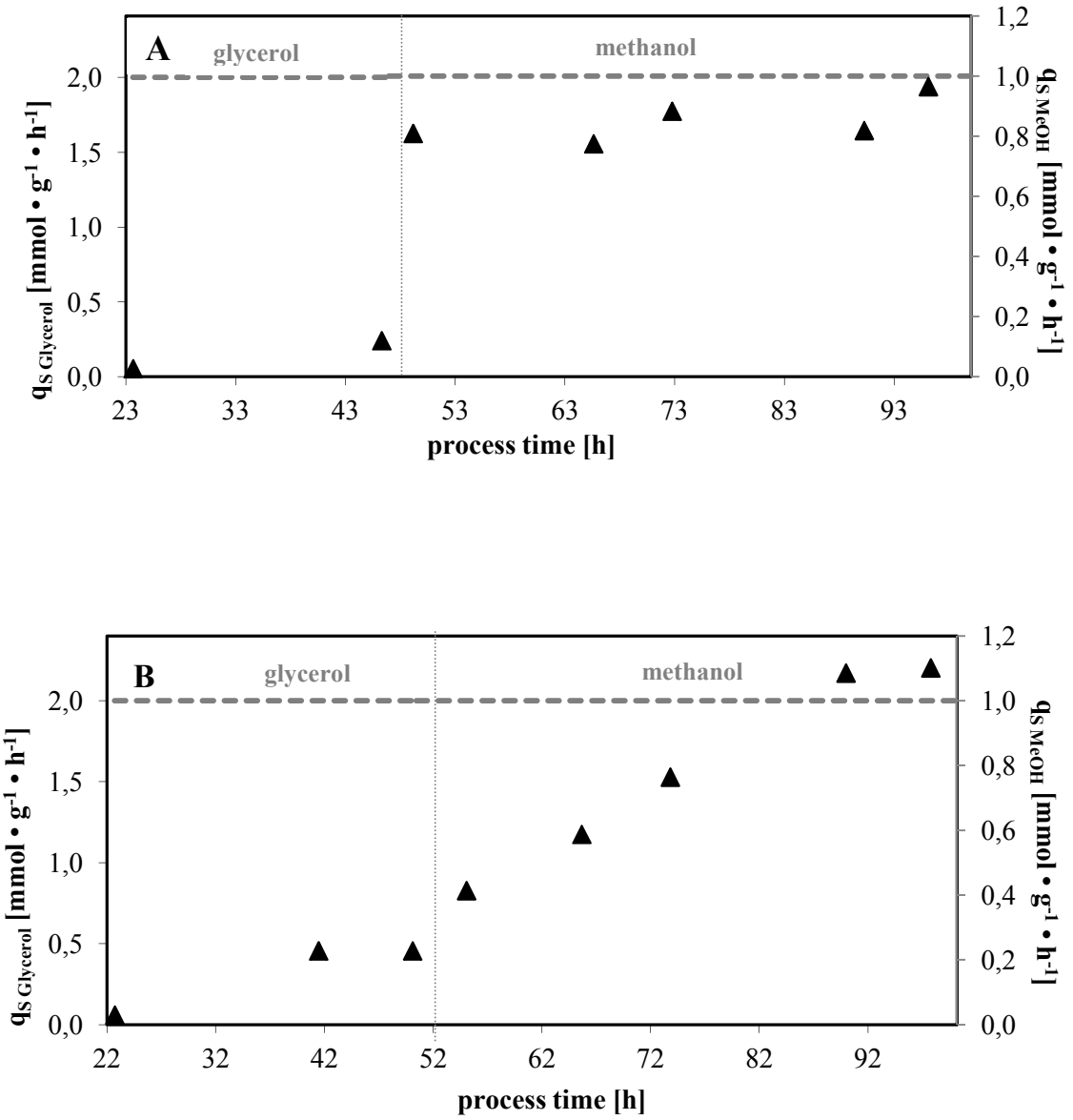

Figure 28: Fermentation of *P.pastoris*. Specific substrate uptake rate (q_S) during glycerol and methanol growth. ▲ q_S observed - - - q_S desired; A, strain CBS7435 expressing wild type HRP C1A; B, strain CBS7435 expressing glycoengineered HRP_N57S.

The strain expressing the glycoengineered variant HRP_N57S showed significantly decreased q_S values at the beginning of the methanol fed-batch phase (Figure 28B). Notably, the adaption time was also two-fold higher compared to the strain expressing the wild type enzyme. One can speculate that these differences in methanol utilization may be caused by unequal metabolic stress resulting from the production of the two different enzyme variants.

In the late induction phase low amounts of methanol were accumulated in both fermentations, indicating that the cells were cultivated close to the limit q_{S_max}, a strain specific parameter which was assumed to be 1 mmol g^{-1} h^{-1} from literature [16, 24] and not determined separately.

Table 16: Fermentation of *P.pastoris.* C-balances. Strain CBS7435 expressing wild type HRP C1A vs. glycoengineered HRP_N57S.

C-source	HRP variant	overall C-balance
glycerol	wild type HRP	1.09
methanol		1.02
glycerol	HRP N57S	0.92
methanol		1.02

Table 16 shows the overall C-balances when *P. pastoris* CBS7435 expressing different HRP variants was utilizing the two C-sources glycerol and methanol. For both strains, the balances are close to one, indicating that all the C-atoms which were fed into the bioreactor could be successfully found again in either the biomass or CO_2 or accumulated methanol and no C-atoms were inexplicably lost (e.g. in undesired metabolites, due to cell lysis).

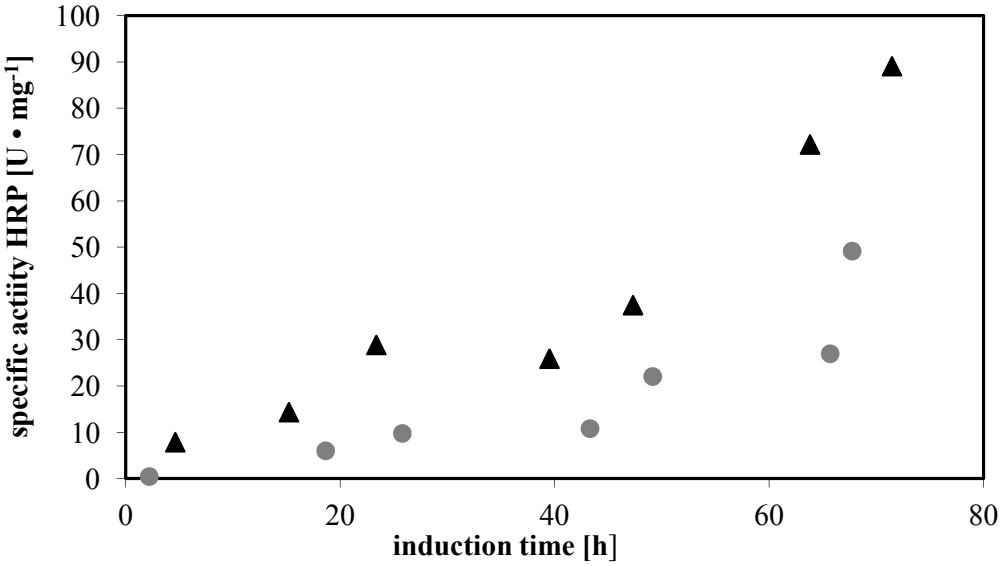

Figure 29: Fermentation of *P. pastoris.* Specific activities during induction phase. ● wild type HRP C1A expressed in strain CBS7435 ▲ glyoengineered HRP_N57S expressed in strain CBS7435. Samples were taken at different timepoints during fermentation and HRP activity was determined photometrically using the substrate ABTS and protein contents were measured by the Bradford assay and specific activities were calculated.

The product-related parameter specific activity of the Serine-substituted HRP enzyme (Figure 29) was up to 2.7-fold increased. Furthermore, the volumetric activity of the glycoengineered rHRP variant peaked at approximately 40 U/mL, an outstanding high value compared to other experiments within this working group, where HRP was frequently applied as reporter enzyme for different bioprocess development experiments in *P. pastoris* before [16, 23, 24, 33].

An experienced bioprocess engineer might say, the exceptional HRP activity is due to the high cell density of this culture or multiple copy integration of the HRP gene, but as a result from biochemical characterization this will turn out to be not true (Chapter „Biochemical characterization“) and can also be seen in specific productivity values, which also considers the biomass concentration.

Summarizing, the outstanding activity of the glycoengineered rHRP variant leads to the following hypotheses:

The strain expressing the mutated enzyme variant HRP_N57S

a. is a better producer (e.g. multiple copy integration)
b. secretes less impurities than the wild type HRP expressing strain
c. generates a more active enzyme (which is in fact a property of the enzyme itself, not of the host strain)

To evaluate the strain perfomances, product-specific parameters were related to the biomass and specific productivities (volumetric / specific, regarding both protein content and HRP activity) were calculated.

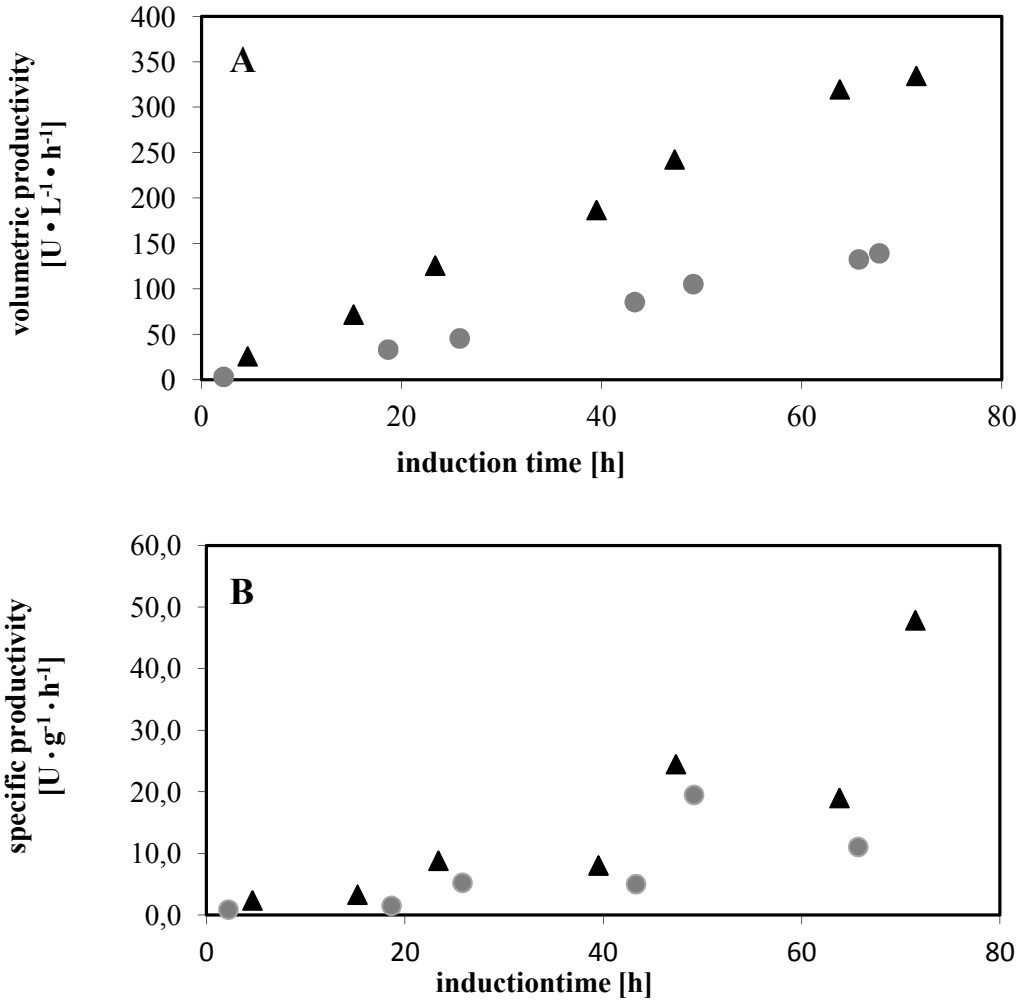

Figure 30: Fermentation of *P.pastoris:* A, volumetric productivity and B, specific productivity (q_P) during induction phase. ● strain CBS7435 expressing wild type HRP C1A; ▲ strain CBS7435 expressing glycoengineered HRP_N57S.

The specific productivity of the wild type variant shows similar values as observed in dynamic fed batch experiments before [16]. The volumetric productivity is a highly interesting parameter for industrial protein expression strains and was subject of a recent study [23], where a maximum of volumetric producivity (~ 50 $U \cdot L^{-1} \cdot h^{-1}$) was achieved by co-overexpressing MUT pathway enzymes. Here, this parameter was significantly improved by a single amino acid substitution. In terms of both, volumetric and specific productivity, the strain expressing the glycoengineered rHRP variant performed significantly better (approx. 2.5-fold increase compared to the wild type expressing strain) (Figure 30) and reached a

maximum value of approx. 350 $U \cdot L^{-1} \cdot h^{-1}$, which is clearly many times higher as described by Krainer et al [23].

However, the outstanding performance of this strain was achieved in a different approach, namely engineering the target protein, not the host strain itself.

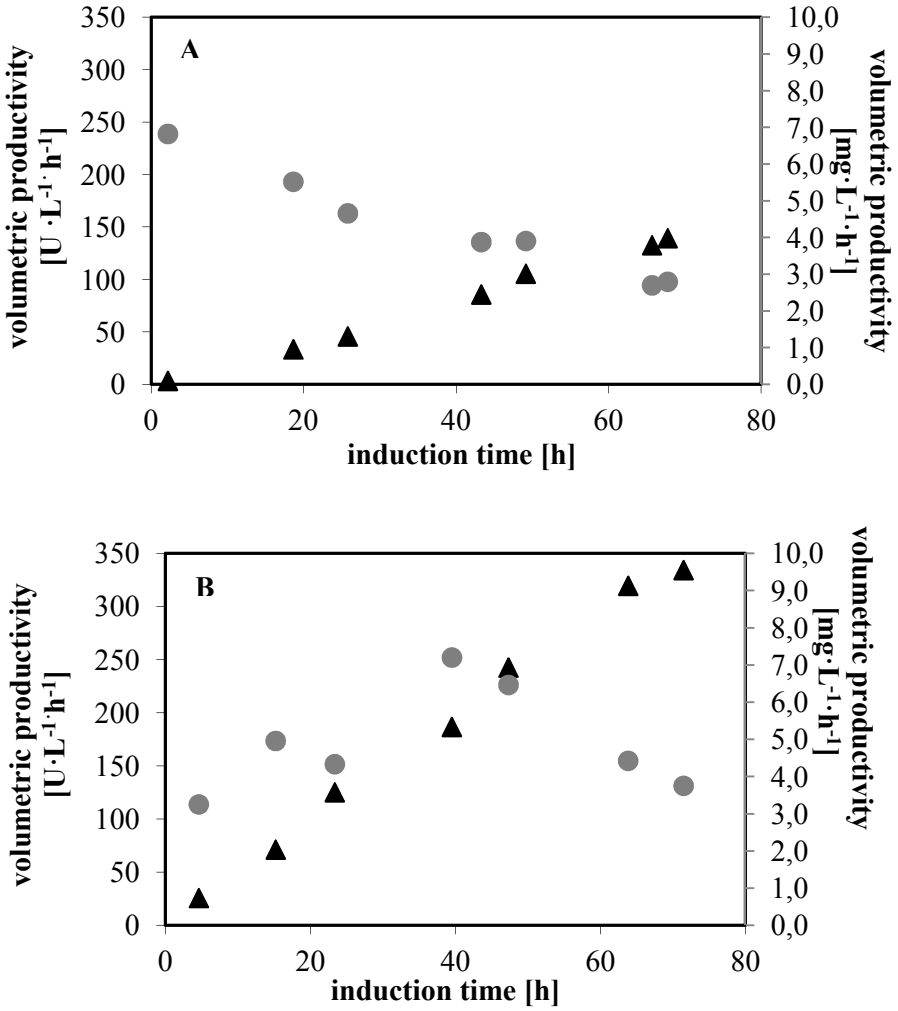

Figure 31: Fermentation of *P. pastoris.* Volumetric productivities regarding total protein content (●) and HRP activity (▲). A, strain CBS7435 expressing wild type HRP; **B**, strain CBS7435 expressing glycoengineered HRP_N57S.

The total protein expression profiles of the two strains were somehow different, as the glycoengineered strain's volumetric protein productivity increased slowly at the beginning of the induction phase, whereby the wild type strain's profile was decreasing. Nevertheless, volumetric productivities concerning HRP activity of both strains continued increasing

constantly (Figure 31). One could link the slower protein productivity of the HRP_N57S – expressing strain to the longer adaption time and decelerated methanol utilization in the early induction phase (Figure 28), however at the end of the fermentation, this strain showed better productivities as the wild type producing strain.

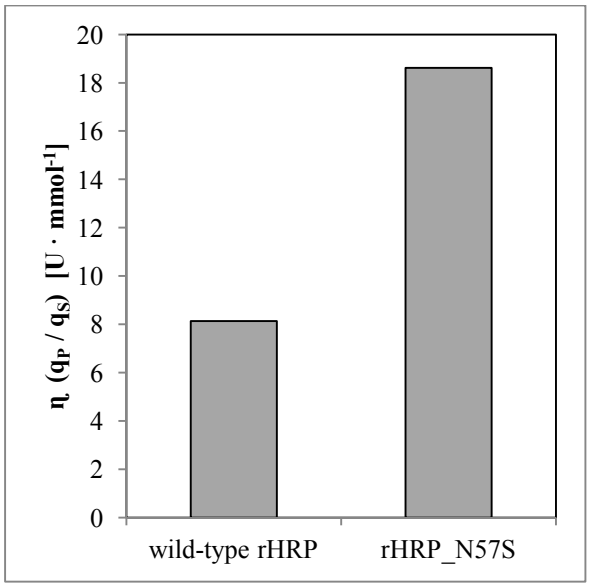

Figure 32: Fermentation of *P. pastoris.* Comparison of average efficiency factors (η) of strain CBS7435 expressing different rHRP variants (wild type and N57S). The efficiency factor η was calculated from averaged rates q_P and q_S during induction phase and describes the efficiency of converting the substrate methanol into product.

As a measure of substrate consumption in relation to product formation, the efficiency factor η was calculated (Figure 32). The engineered strain expressing rHRP_N57S showed a 2.3-fold higher efficiency compared to the wild type enzyme and also exceeded the values that have been described earlier [23] , who reported max. η-values of approx. 3.

However, both fermentations showed similar bioprocess characteristics which was particularly important for the comparison of the two enzyme variants itself, as the glycosylation is strongly dependent on the cultivation conditions [18] and sufficient enzyme amounts were generated for subsequent purification and characterization studies.

3.3.5 Purification of rHRP from fermentations

After harvesting the fermentation broth, cells were removed by a simple centrifugation and/or filtration step, which is a exceptional advantage of protein production in *P.pastoris* as the target protein remains in the supernatant. The rebuffered crude extracts were purified by the fast and efficient 2-step protocol described in the first chapter of this thesis. After the first step, HCIC purification, both enzyme solutions were purified 5-6 fold in the flowthrough, resulting in a specific activity of around 400 U/mg. After a polishing step applying CIM-DEAE, the specific activity was 800 U/mg. Hence, the crude fermentation supernatant was purified up to 12-fold by applying this simple 2-step protocol. The enzyme solutions were successfully purified and had a final specific activity of around 800 U/mg after applying the novel 2-step purification protocol.

3.3.6 Characterization of rHRP variants

3.3.6.1 pH stability

The purified and concentrated enzyme solutions were diluted to approximately 1.5 U/mL in different buffer systems. After incubation, the catalytic activity was measured. According to Figure 33, the pH optimum for wild type rHRP is between pH 5 and 10, for the mutant HRP N57S from pH 5.5 to 9.0. Interestingly, the mutated variant is more stable at acidic pH values. At a pH of 3.5, more than 50% of the maximum activity is detected, whereby the wild type rHRP is inactivated (<50% resiudal activity). Even though the mutated variant has slighlty decreased catalytic activity at higher pH values compared to the wild type enzyme, it is still above 70% of initial activity. Both rHRP variants are stable at physiological pH values, which is important for medical applications. However, the final enzyme variant for *in vivo* uses must not contain immunogenic sugar chains such as Mannose residues, which are still present in both enzyme variants described here.

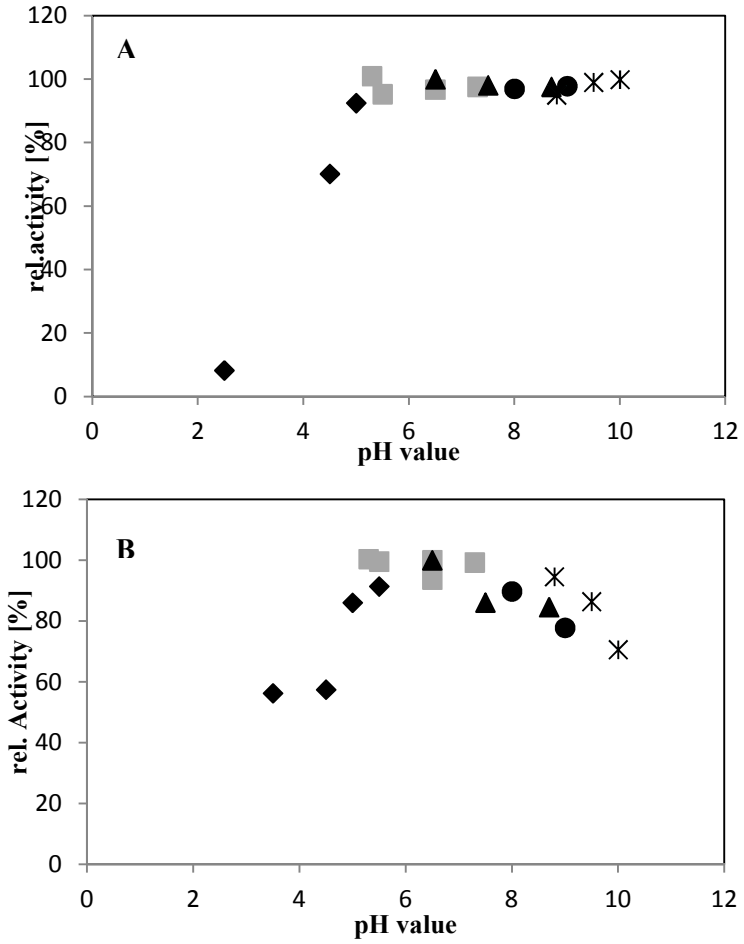

Figure 33: pH Stability of different rHRP variants expressed in *P. pastoris* CBS7435. A, wild type rHRP**, B,** HRP N57S**.** The enzyme preparations was incubated in different 50 mM buffers at 30°C for 30 min before the remaining enzymatic activity was determined photometrically ◆ Citrate, ■ Carbonate, ▲ Phosphate, ● Tris, ✱ Glycine; all buffers were 50 mM.

3.3.6.2 Biochemical characterization

To determine the kinetic parameters K_M and k_{cat} for the substrate ABTS, HRP activity was measured using the reducing substrate ABTS and H_2O_2 as a saturating substrate. Michaelis Menten plots of both enzyme variants, wild type rHRP and rHRP_N57S, are shown in Figure 34 and Figure 35.

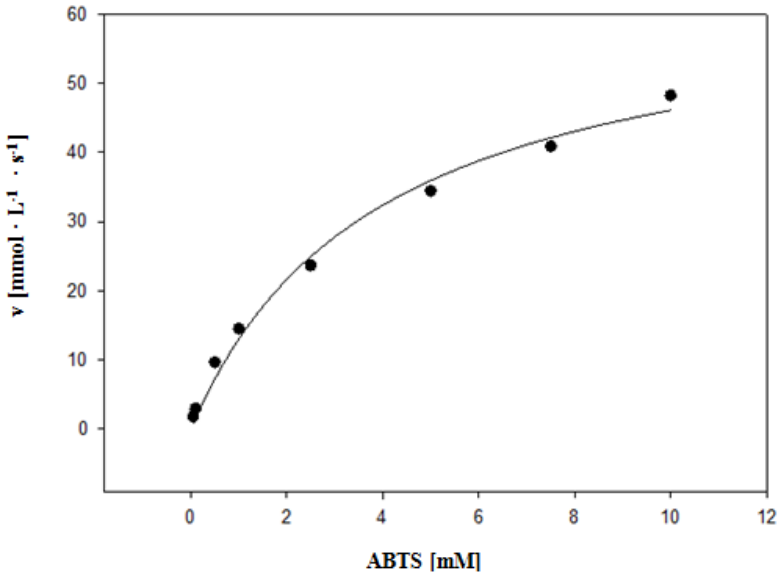

Figure 34: Michaelis-Menten plot of wild-type HRP using the substrate ABTS.

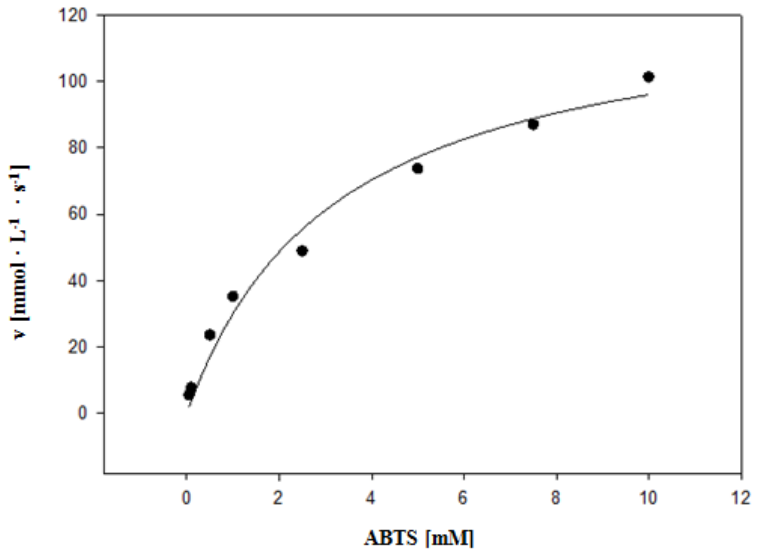

Figure 35: Michaelis-Menten plot mutated enzyme variant HRP_N57S using the substrate ABTS.

Table 17: Kinetic parameters of rHRP variants.

Kinetic parameter	Wild-type HRP	HRP_N57S
K_M [mM]	3.93	3.21
k_{cat} [s^{-1}]	69.57	137.32
k_{cat}/K_M [$mM \cdot s^{-1}$]	17.7	42.78

As visible in Table 17, both enzyme variants have similar K_M values for ABTS, meaning that both have the same affinity to the reducing substrate. An outstanding result is the two-fold higher value for k_{cat} of the Serine-substituted version of rHRP. Moreover, the catalytic efficiency of the mutated enzyme is significantly higher (*i.e.* it can convert a magnitude more substrate molecules as the wild type enzyme in the same timespan). This amino acid substitution from Asparagin to Serin has apparently improved the enzyme's catalytic activity dramatically, which makes this version an excellent candidate for industrial applications such as diagnostic kits or biosensors, which require high sensitivity and efficient catalytic activity.

3.3.6.3 Glycosylation analysis

The potential use of HRP in medicine requires detailed knowledge of the enzyme's glycan structure, as it may influence active pharmaceutical ingredient clearance dramatically and can cause severe adverse reactions in the human body [20]. Thus, the glycosylation of a recombinant protein for therapeutic use must be investigated extensively. Purified rHRP enzyme variants (wild type and N57S-substituted mutant) were subjected to glycosylation analysis by digestion with different enzymes and resulting peptides were analyzed using liquid chromatography – electrospray ionization – mass spectrometry (LC-ESI-MS).

Tryptic peptides did not afford any sequence annotation for theoretical peptides of both, wild type and mutated enzymes, probably due to the extensive and heterogenic glycosylation of rHRP from *P. pastoris* or the presence of other post-translational modifications such as

phosphorylation [19] and of course, the large number of glycosylation sites complicating the analysis even more. Another difficulty may have been the cleavage by the protease, resulting not in the predicted peptides but a complex pattern which could not be solved using automated calculations. However, typical hexose mass increments were observed in MS spectra indicative for >10 mannose residues but could not be assigned to defined peptides, underlining the complexity of the glycosylation within the HRP molecule once again.

Another successful approach to determine glycan structures is to search for the deglycosylated peptide as the glycosylated one will elute in the vicinity when separated by reversed phase (RP)-LC [45]. However, an enzymatic deglycosylation using PNGase A did not help to identify the deglycosylated peptide harbouring the site N57 within the wild type enzyme variant (data not shown). Even though the N57S enzyme could be identified (*vide infra*), the elution profile may be somewhat different, as another amino acid residue alters the retention profile on RP and thus gave no useful information for the glycosylated HRP species of the wild type variant, the one having an intact *N*-glycosylation site (Asn-X-Thr). Thus, this data could not be used for the determination of the glycosylation of site N57 in the wild type enzyme expressed in *P.pastoris*.

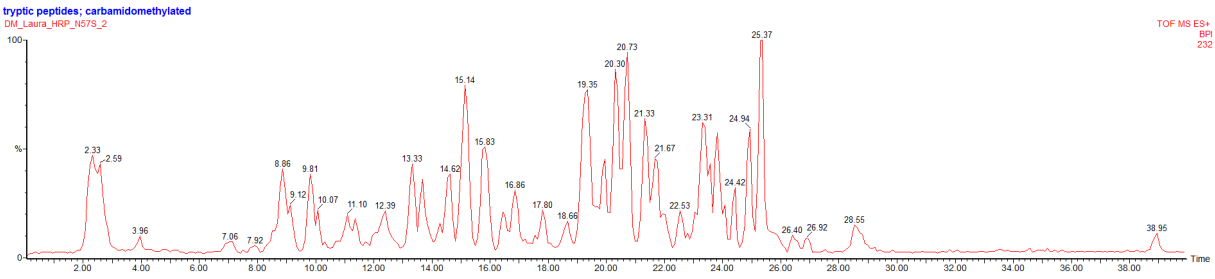

Figure 36: LC separation of a chymotryptic digest of rHRP_N57S. Chymotryptic peptides were loaded onto a RP-column and eluted in a defined gradient of acetonitrile and analyzed on a Q-TOF instrument.

However, for the mutated variant HRP_N57S, a chymotryptic digest allowed the identification of a peptide at site 57 of the sequence LD**S**TTSF eluting at LC-retention time 15.6 min (Figure 36) harbouring a protonated molecule ion at *m/z* 770.357. Notably, this peptide resulted from a missed cleavage by the enzyme Chymotrypsin.

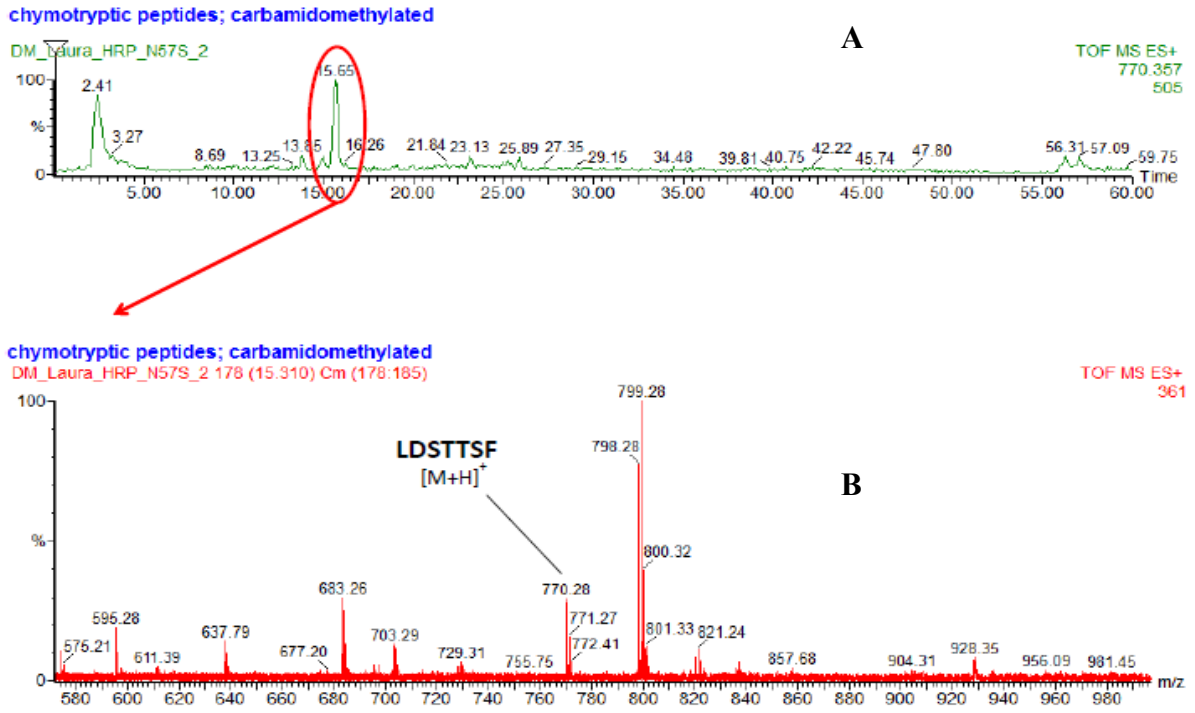

Figure 37: LC-ESI-MS analysis of HRP_N57S. A miscleaved peptide at site 57 in the rHRP variant N57S was suspected to appear at *m/z* of 770.357 corresponding to a protonated molecule ion of the sequence LD**S**TTSF. A. selected ion chromatogramm B. MS spectrum of the selected peptide at retention time 15.6.

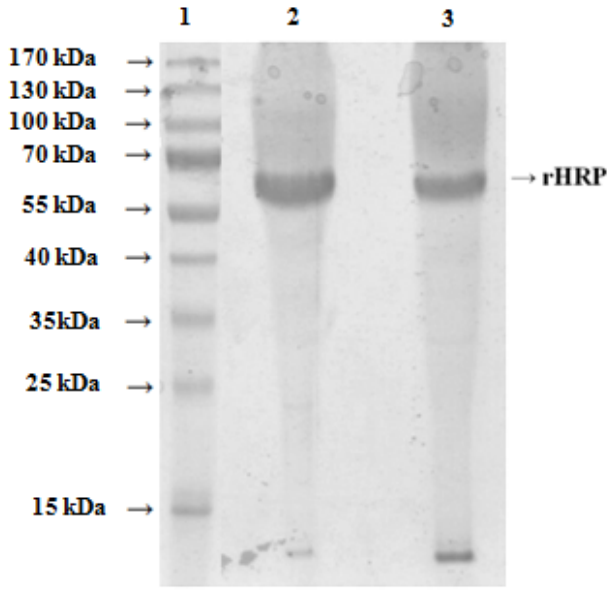

Figure 38: SDS-PAGE of final enzyme preparations for glycosylation analysis. Purified enzyme solutions expressed in *P. pastoris* CBS7435 in a bioreactor under well-defined cultivation conditions visualized on the here presented SDS-PAGE were subjected to LC-ESI-MS. Lane 1, molecular weight marker (2 µg); lane 2, wild-type rHRP (10 µg); lane 3, HRP_N57S (10 µg).

There were also other masses present in the MS spectrum of the corresponding peptide at LC-retention time l5.6 (Figure 37). This may result from impurities that eluted concomitantly with the N57S-peptide as the sample was not purified from a gel single band, but digested in solution and measured directly. According to SDS-PAGE, there are also minor contaminating proteins present in the enzyme solutions (Figure 38), even if the target protein was accounting for >90% of the total protein content after purification. Moreover, the sum of a LC peak hardly ever represents a single peptide species. Hence, *m/z* values other than 770.357 can be assigned to impurities within the enzyme solution or unidentified co-eluting peptides.

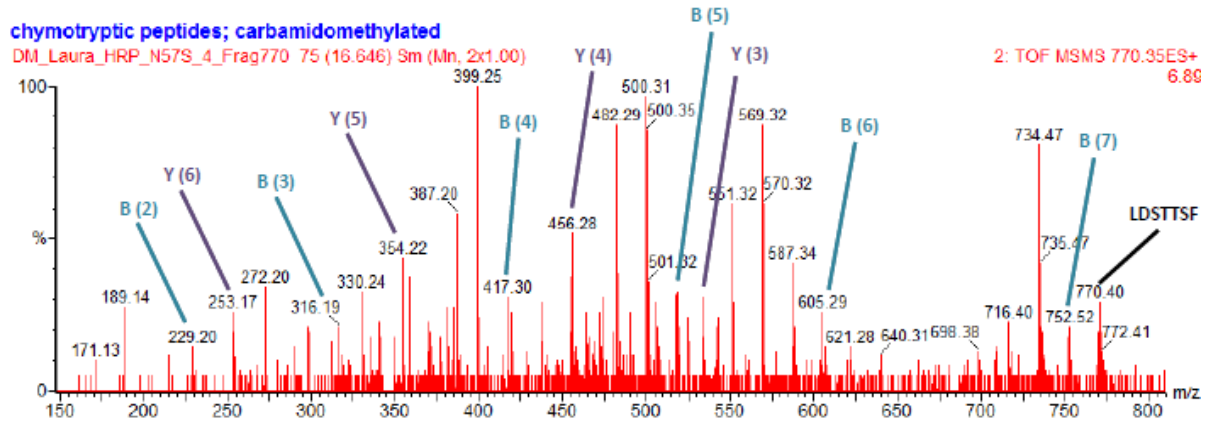

Figure 39: MS/MS analysis of the peptide LDSTTSF. The molecule ion from the N57S peptide (*m/z* 770.35) was selected for CID fragmentation and analyzed on a Q-TOF MS. Fragment ions were annotated using the web tool "Fragment Ion Calculator".

Anyway, this peptide was further fragmented and analyzed by *de novo* sequencing in a MS/MS approach. Fragment ions resulting from collision induced dissociation (CID) were annotated as b- and y-ion species (6/7, 4/7 respectively) (Figure 39) from a non-glycosylated peptide, being the confirmation for the correct mass of the miscleaved peptide of the sequence LDSTTSF at site 57 within rHRP_N57S.

As a conclusion, the mutated HRP variant N57S was confirmed to be correctly expressed in the host *P. pastoris* in a less glycosylated form. The identification of the original glycosylation pattern (before introducing the mutation and thereby removing the glycosylation site N57) could not be solved in a straight-forward approach and must be investigated in more detail, but this was beyond the scope of this thesis.

3.4 Conclusions

Altering the amino-acid sequence of rHRP has already shown some success in terms of stability and catalytic activity (e.g. [6, 46]) and aided the understanding of the catalytic function of individual amino acids within the HRP molecule.

Horseradish peroxidase expressed in *P. pastoris* is hyperglycosylated, which hampers a straight forward conventional purification [15, 17] and causes immunogenic responses in the human body when the enzyme should be applied for *in vivo* medical applications [10]. Thus, HRP was glycoengineered by substituting the *N*-glycosylation recognition site N57 to three structural similar amino-acids in a PCR-based methodology. After propagation of the plasmid in *E. coli*, the gene for HRP was introduced into different *P. pastoris* strains which were subsequently screened for expressing clones. A protease deficient strain was not able to express the enzyme in an active form in substantial amounts, which is why the plasmid was transformed into the strain it was designed for (CBS7435). Hence, the combination of a vector in a non-familiar host strain should be avoided and dedicated plasmids must be used in order to guarantee correct integration into the *Pichia* genome.

Another interesting observation was the impact of a single substitution in the amino-acid chain, which caused a metabolic collapse of the host cell when grown on methanol. This was observed for a Aspartat-substituted mutant only, showing the significant change in enzyme assembly when a single amino acid is substituted.

However, the best enyme variant HRP_N57S was expressed in a controlled environment in a bioreactor to assure comparable cultivation conditions and to obtain sufficient enzyme amounts for subsequent biochemical characterization and glycosylation analysis. Finally, the Serine substituted mutant showed more than 2.5-fold higher catalytic activity and a higher thermal stability. These results illustrate the power of molecular manipulations to improve an industrial important enzyme by solely substituting a single amino acid.

LC-ESI-MS analysis confirmed the absence of *N*-glycosylation at site N57S, but the authentic glycosylation was not solved yet and more efforts must be assigned to approach this problem.

4 Overall Conclusions

Due to the wide range of applications in industry and medicine, HRP is subject of numerous studies in biotechnology. Specially the recombinant production of the enzyme would allow cost-reduced and well-defined enzyme preparations. Appropriate host organisms are hard to find for the expression of this complex molecule due to their inability of synthesizing the enzyme in an active form or giving insufficient yields for an economical process. Moreover, the demand of less-glycosylated HRP has not yet been satisfied.

P.pastoris ***as a expression host for glycosylated HRP variants and the purification problem***

The yeast *P. pastoris* has been proved useful for large-scale heterologous protein production and is capable of performing all post-translational modifications of a higher eukaryote. Thus, this system was superior to express HRP recombinantly. However, the extensive glycosylation of *P. pastoris* hampers an efficient conventional purification process. This problem was solved by applying a fast and efficient 2-step purification protocol which was further improved using a mixed-mode resin (HCIC) as a first step, and a monolithic column (CIM-DEAE) for polishing. Using this method, rHRP could be purified more than 10-fold operating both systems in a negative mode providing an efficient and easy-to-do preparative purification of the hyperglycosylated enzyme expressed in *P. pastoris*. This system can be applied for different recombinant hyperglycosylated proteins from this methylotrophic yeast and was subject of research for the purification of different HRP isoenzymes at the Technical University of Vienna and Graz at the time of rewriting this thesis. Recently, the here developed purification protocol was applied for the purification of 19 HRP isoenzymes, which showed even greater success for other isoforms than HRP C1A. The results were published in March 2014 [47]. Hence, the here developed 2-step purification strategy has already been

proved successful also for other rHRP isoenzymes and thus, is a valuable tool for the recombinant production of HRP or in general, for hyperglycosylated proteins produced in *P.pastoris*.

Removing the N-glycosylation site N57

In a molecular biology approach, one of the eight *N*-glycosylation sites was removed by substituting the amino acid Asparagine at site N57 with the three structural similar residues Aspartat, Glutamine and Serine. The most beneficial mutation turned out to be Serine, which improved the enzyme's catalytic activity more than 2-fold and increased the thermostability compared to both, the plant and the recombinant wild type enzyme from *P. pastoris*. The mutated rHRP variants were expressed in large scale fed-batch fermentations, purified applying the previously developed 2-step purification protocol and characterized thoroughly. Finally, the removal of a *N*-glycosylation site and the substitution of Asparagine by a Serine residue at site N57 was confirmed by a mass spectrometry approach applying LC-ESI-MS. The final enzyme variant is an excellent candidate for industrial purposes such as waste water treatment or medical diagnostic kits. Moreover, due to the high stability but more the extraordinary catalytic activity, the mutated enzyme variant represents a valuable enzyme for high sensitivity bioassays.

The here developed methodology will be used for removing the residual *N*-glycosylation sites within the recombinant HRP molecule from *P. pastoris* which should result in a deglycosylated but improved enzyme variant, that will be tested for potential applications in targeted cancer therapies.

5 Outlook

As the experiments with the monolithic columns were very promising, the second step of the here presented purification protocol will be investigated in a DoE approach and scaled-up to be available for large scale purifications.

Moreover, within the HRP glycoengineering project (FWF P24861-B19) there are 7 other *N*-glycosylation sites currently under investigation, which will be removed applying the same methodology as described in this thesis. The final enzyme variant will be a combination of the most beneficial mutations or *N*-glycosylation will be totally removed in order to obtain a non-glycosylated fully active enzyme variant, which will be applied for targeted cancer therapies at the University of Oxford, England and Christchurch, New Zealand. The final enzyme will be tested in mammalian cell cultures for a potential application in promising therapeutic approaches.

Additionally, there were more than 27 isoenzymes identified recently at the Technical University of Graz, which will be characterized in detail in order to have a set of different rHRP preparations available for diagnostic and medical purposes.

6 Abbreviations

a, b	left and right distance from peak center at 10 % peak height
ABTS	2.2' azino bis 3-ethylbenzthiazoline-6-sulphonic acid
AC	affinity chromatography
AEX	anion exchange chromatography
AF	asymmetry factor
AOX	Alcohol oxidase
BSA	bovine serum albumin
CER	Carbondioxide Evolution Rate [mmol · L^{-1}· h^{-1}]
CEX	cation exchange chromatography
CID	Collision Induced Dissociation
CIM-DEAE	Convective Interactive Media – Diethylaminoethyl
ConA	Concavanalin A
CV	Column volumes
δ -Ala	δ-Aminolevulinic acid
DHAS	Dihydroxyacetone synthase
DoE	Design of Experiments
DTT	Dithiothreitol
Fuc	Fucose
GlcNAc	N-acetylglucosamine
GOI	Gene of interest
H_2O_2	hydrogen peroxide
HCIC	hydrophobic charge induction chromatography
HETP	height equivalent of a theoretical plate
HRP	horseradish peroxidase
IAA	indole-3-acetic acid
IEF	isoelectric focussing

k_{cat}	Catalytic constant [s^{-1}]
kDa	Kilodalton
K_M	Michaelis-Menten Constant [mmol · L^{-1}]
L	column length (in cm for HETP, in m for N/m)
LB	Luria-Bertani
LC-ESI-MS	Liquid chromatography-electrospray ionization-mass spectrometry
Man	Mannose
mAU	Milli Absorbance Units
MEP	4-Mercapto-ethyl-pyridine
MOPS	4-Morpholinepropanesulfonic acid
Mut^-	methanol utilization minus
Mut^+	methanol utilization plus
Mut^S	methanol utilization slow
(m)V	(Milli) Volt
MW	Molecular weigth [kDa]
N/m	theoretical plates per meter
OD_{600}	Optical density at 600 nm
PF	purification factor
pI	isoelectric point
PID	proportional-integral-derivative
q_P	Specific productivity [U · g^{-1} · h^{-1}] or [g · g^{-1} · h^{-1}]
q_S	Specific substrate uptake rate [mmol · g^{-1} ·h^{-1}]
rHRP	recombinant horseradish peroxidase
SEC	size exclusion chromatography
SoE	Splicing by overlap extension
v_{max}	Maximum reaction velocity
$Y_{x/s}$	Yield biomass to substrate [g/g]
μ	Specific growth rate [h^{-1}]

7 Tables and Figures

8 References

1. Veitch, N.C., *Horseradish peroxidase: a modern view of a classic enzyme.* Phytochemistry, 2004. **65**(3): p. 249-259.
2. Smith, A.T., et al., *Expression of a Synthetic Gene for Horseradish Peroxidase-C in Escherichia-Coli and Folding and Activation of the Recombinant Enzyme with Ca-2+ and Heme.* Journal of Biological Chemistry, 1990. **265**(22): p. 13335-13343.
3. Gajhede, M., et al., *Crystal structure of horseradish peroxidase C at 2.15 angstrom resolution.* Nature Structural Biology, 1997. **4**(12): p. 1032-1038.
4. Bandyopadhyay U., S.A., Banerjee R.K., *Role of Active Site Residues in Peroxidase Catalysis: Studies on Horseradish Peroxidase.* PINSA, 1999. **65**(5): p. 315-330.
5. Tams, J.W. and K.G. Welinder, *Mild Chemical Deglycosylation of Horseradish-Peroxidase Yields a Fully Active, Homogeneous Enzyme.* Analytical Biochemistry, 1995. **228**(1): p. 48-55.
6. Smith, A.T., et al., *Characterisation of a haem active-site mutant of horseradish peroxidase, Phe41----Val, with altered reactivity towards hydrogen peroxide and reducing substrates.* Eur J Biochem, 1992. **207**(2): p. 507-19.
7. Ryan, B.J. and C. O'Fagain, *Effects of mutations in the helix G region of horseradish peroxidase.* Biochimie, 2008. **90**(9): p. 1414-1421.
8. Asad, S., K. Khajeh, and N. Ghaemi, *Investigating the Structural and Functional Effects of Mutating Asn Glycosylation Sites of Horseradish Peroxidase to Asp.* Applied Biochemistry and Biotechnology, 2011. **164**(4): p. 454-463.
9. Ryan, O., M.R. Smyth, and C.O. Fagain, *Horseradish peroxidase: the analyst's friend.* Essays Biochem, 1994. **28**: p. 129-46.
10. Folkes, L.K. and P. Wardman, *Oxidative activation of indole-3-acetic acids to cytotoxic species - a potential new role for plant auxins in cancer therapy.* Biochemical Pharmacology, 2001. **61**(2): p. 129-136.
11. Candeias, L.P., et al., *Rates of reaction of indoleacetic acids with horseradish peroxidase compound I and their dependence on the redox potentials.* Biochemistry, 1996. **35**(1): p. 102-8.
12. Lavery, C.B., et al., *Purification of Peroxidase from Horseradish (Armoracia rusticana) Roots.* Journal of Agricultural and Food Chemistry, 2010. **58**(15): p. 8471-8476.
13. Greco, O., et al., *Development of a novel enzyme/prodrug combination for gene therapy of cancer: horseradish peroxidase/indole-3-acetic acid.* Cancer Gene Therapy, 2000. **7**(11): p. 1414-1420.
14. Hartmann, C. and P.R.O. Demontellano, *Baculovirus Expression and Characterization of Catalytically Active Horseradish-Peroxidase.* Archives of Biochemistry and Biophysics, 1992. **297**(1): p. 61-72.
15. Morawski, B., et al., *Functional expression of horseradish peroxidase in Saccharomyces cerevisiae and Pichia pastoris.* Protein Engineering, 2000. **13**(5): p. 377-384.
16. Dietzsch, C., O. Spadiut, and C. Herwig, *A dynamic method based on the specific substrate uptake rate to set up a feeding strategy for Pichia pastoris.* Microbial Cell Factories, 2011. **10**: p. 14.
17. Spadiut, O., et al., *Purification of a recombinant plant peroxidase produced in Pichia pastoris by a simple 2-step strategy.* Protein Expr Purif, 2012. **86**(2): p. 89-97.

18. Li, P., et al., *Expression of recombinant proteins in Pichia pastoris.* Appl Biochem Biotechnol, 2007. **142**(2): p. 105-24.
19. Bretthauer, R.K. and F.J. Castellino, *Glycosylation of Pichia pastoris-derived proteins.* Biotechnol Appl Biochem, 1999. **30 (Pt 3)**: p. 193-200.
20. Cereghino, J.L. and J.M. Cregg, *Heterologous protein expression in the methylotrophic yeast Pichia pastoris.* Fems Microbiology Reviews, 2000. **24**(1): p. 45-66.
21. Montesino, R., et al., *Variation in N-linked oligosaccharide structures on heterologous proteins secreted by the methylotrophic yeast Pichia pastoris.* Protein Expr Purif, 1998. **14**(2): p. 197-207.
22. Trimble, R.B., et al., *Structure of oligosaccharides on Saccharomyces SUC2 invertase secreted by the methylotrophic yeast Pichia pastoris.* J Biol Chem, 1991. **266**(34): p. 22807-17.
23. Krainer, F.W., et al., *Recombinant protein expression in Pichia pastoris strains with an engineered methanol utilization pathway.* Microbial Cell Factories, 2012. **11**: p. 22.
24. Dietzsch, C., O. Spadiut, and C. Herwig, *A fast approach to determine a fed batch feeding profile for recombinant Pichia pastoris strains.* Microbial Cell Factories, 2011. **10**: p. 85.
25. Hartner, F.S., et al., *Promoter library designed for fine-tuned gene expression in Pichia pastoris.* Nucleic Acids Research, 2008. **36**(12): p. e76.
26. Romanos, M.A., C.A. Scorer, and J.J. Clare, *Foreign Gene-Expression in Yeast - a Review.* Yeast, 1992. **8**(6): p. 423-488.
27. Fraguas, L.F., F. Batista-Viera, and J. Carlsson, *Preparation of high-density Concanavalin A adsorbent and its use for rapid, high-yield purification of peroxidase from horseradish roots.* Journal of Chromatography B-Analytical Technologies in the Biomedical and Life Sciences, 2004. **803**(2): p. 237-241.
28. Helmholz, H., et al., *Process development in affinity separation of glycoconjugates with lectins as ligands.* Journal of Chromatography A, 2003. **1006**(1-2): p. 127-135.
29. Brattain, M.G., M.E. Marks, and T.G. Pretlow, *Purification of Horseradish-Peroxidase by Affinity Chromatography on Sepharose-Bound Concanavalin-A.* Analytical Biochemistry, 1976. **72**(1-2): p. 346-352.
30. Miranda, M.V., et al., *The extractive purification of peroxidase from plant raw materials in aqueous two-phase systems.* Acta Biotechnologica, 1998. **18**(3): p. 179-188.
31. Guo, W. and E. Ruckenstein, *Separation and purification of horseradish peroxidase by membrane affinity chromatography.* Journal of Membrane Science, 2003. **211**(1): p. 101-111.
32. Bhatti, H.N., M.N. Akbar, and M.A. Zia, *Kinetics of irreversible thermal denaturation of horseradish peroxidase.* Journal of the Chemical Society of Pakistan, 2007. **29**(2): p. 99-102.
33. Zalai, D., et al., *A dynamic fed batch strategy for a Pichia pastoris mixed feed system to increase process understanding.* Biotechnology Progress, 2012: p. DOI: 10.1002/btpr.1551.
34. Passarinha, L.A., et al., *A new approach on the purification of recombinant human soluble catechol-O-methyltransferase from an Escherichia coli extract using hydrophobic interaction chromatography.* Journal of Chromatography A, 2008. **1177**(2): p. 287-96.
35. Huang, C.J., et al., *A proteomic analysis of the Pichia pastoris secretome in methanol-induced cultures.* Applied Microbiology and Biotechnology, 2011. **90**(1): p. 235-47.
36. Arnold, F. and L. Zhanglin, *Expression of functional eukaryotic proteins.* US Patent Application Publication, 2003.

37. Yasuda, K., et al., *Efficient and rapid purification of recombinant human alpha-galactosidase A by affinity column chromatography.* Protein Expression and Purification, 2004. **37**(2): p. 499-506.
38. Iberer, G., et al., *Improved performance of protein separation by continuous annular chromatography in the size-exclusion mode.* Journal of Chromatography A, 2001. **921**(1): p. 15-24.
39. Podgornik, H. and A. Podgornik, *Separation of manganese peroxidase isoenzymes on strong anion-exchange monolithic column using pH-salt gradient.* J Chromatogr B Analyt Technol Biomed Life Sci, 2004. **799**(2): p. 343-7.
40. Podgornik, H., et al., *The effect of agitation and nitrogen concentration on lignin peroxidase (LiP) isoform composition during fermentation of Phanerochaete chrysosporium.* J Biotechnol, 2001. **88**(2): p. 173-6.
41. Podgornik, H., A. Podgornik, and A. Perdih, *A method of fast separation of lignin peroxidases using convective interaction media disks.* Anal Biochem, 1999. **272**(1): p. 43-7.
42. Barut, M., et al., *Convective interaction media short monolithic columns: enabling chromatographic supports for the separation and purification of large biomolecules.* J Sep Sci, 2005. **28**(15): p. 1876-92.
43. Invitrogen, *pPiCZalpha A, B and C; Pichia expression vectors for selection on Zeocin™ and purification of secreted,*. 2008.
44. Tams, J.W. and K.G. Welinder, *Glycosylation and thermodynamic versus kinetic stability of horseradish peroxidase.* Febs Letters, 1998. **421**(3): p. 234-236.
45. Pabst, M., et al., *Glycan profiles of the 27 N-glycosylation sites of the HIV envelope protein CN54gp140.* Biol Chem, 2012. **393**(8): p. 719-30.
46. Ryan, B.J. and C. O'Fagain, *Effects of single mutations on the stability of horseradish peroxidase to hydrogen peroxide.* Biochimie, 2007. **89**(8): p. 1029-32.
47. Krainer, F.W., et al., *Purification and basic biochemical characterization of 19 recombinant plant peroxidase isoenzymes produced in Pichia pastoris.* Protein Expression and Purification, 2014. **95**: p. 104-112

9 Appendix

9.1 Enzymes and strains

Phusion® Hot Start High-Fidelity DNA Polymerase 2 U/µL, 5x Phusion HF buffer; Thermo Scientific, USA

***Taq* DNA Polymerase** (recombinant) 5 U/µL, 25 mM MgCl2, 10x *Taq* buffer; Fermentas, Germany

FastDigest® *Eco*RI 1 U/µL, 10x FastDigest® Buffer, 10x FastDigest® green Buffer, `5'G^AATTC3'` / Fermentas, Germany

FastDigest® *Swa*I 1 U/µL, 10x FastDigest® Buffer, 10x FastDigest® green Buffer, `5'G^AATT / AAAT 3'`; Fermentas, Germany

***Sac*I 10 U/µL,** 10 x Tango buffer, 5'G^AGCT / C 3'; Fermentas, Germany

***Escherichia coli* TOP10F':** Invitrogen corporation, San Diego, USA

***P. pastoris* SMD1168H**: Genotype: phenotype: $Mut^{+;}$ proteinase A-deficient; Invitrogen, Carlsbad

***P. pastoris* CBS7435:** Genotype: Δ*aox*1, phenotype: Mut^{S} engineered at Graz University of Technology

9.2 Media, solutions and chemicals

Low-salt LB (Luria-Bertani) (agar), per liter: yeast extract, 5 g**;** 10 g; Bacto™ Peptone, 20 g; Sodium-chloride, 10 g; (Agar-agar, 15 g;); autoclaved.

Terrific broth (TB), per liter: yeast extract, 24 g; Bacto™ Peptone, 12 g; glycerol, 0.4% (v/v); antifoam Struktol, 0.1 mL; KH_2PO_4 buffer, 100 mM (after autoclaving).

YPD (agar), per liter: yeast extract, 10 g; Bacto™ Peptone, 20 g; (Agar agar, 15 g); Glucose monohydrate, 20 g (after autoclaving).

YPD(S) (agar), per liter: yeast extract, 10 g; Bacto™ Peptone, 20 g; Sorbitol, 182.2 g; (Agar agar, 15 g); Glucose monohydrate, 20 g (after autoclaving).

BEDS buffer, per liter: Bicine, 1.636 g; DMSO, 50 mL; Tri-ethyleneglycol, 30 mL; Sorbitol, 182.4 g; pH adjusted to 8.3 with 2 M NaOH; filter-sterilized.

BMGY (**B**uffered **G**lycerol-complex **M**edium**), per liter:** potassium phosphate, pH 6.0, 100 mM; YNB, 1.34 g; Biotin, 4 x 10^{-5}%; glycerol, 1 g; Zeocin^{TM}, 100 µg after autoclaving.

BMMY (**B**uffered **M**ethanol-complex **M**edium)**, per liter:** potassium phosphate, pH 6.0, 100 mM; YNB, 1.34 g; Biotin, 4 x 15-5%, Methanol, 0.5% (v/v); Zeocin^{TM}, 100 µg.

Induction supplements: methanol, 0.5 and 1% of culture volume, δ-Aminolevulinic acid (δ-Ala), 1 mM.

Breaking Buffer, per liter: Sodium Phosphate, 50 mM; EDTA, 1mM; Glycerol, 5%; Protease Inhibitor cocktail, 10 tablets (complete-Mini, EDTA-free; Roche Diagnostics, Germany).

9.3 Bioreactor cultivation media

Preculture: Yeast nitrogen base media (YNBM), per liter: potassium phosphate buffer (pH 6.0), 0.1 M; YNB w/o Amino acids and Ammonia Sulfate (Difco™), 3.4 g; $(NH_4)_2SO_4$, 10 g; biotin, 400 mg; glucose, 20 g, Zeocin^{TM} (100 ng/µL)

Batch/fed batch: Basal salt media (BSM), per liter: 85% phosphoric acid, 26.7 mL; $CaSO_4 \cdot 2H_20$, 1.17 g; K_2SO_4, 18.2 g; $MgSO_4 \cdot 7H_2O$, 14.9 g; KOH, 4.13 g; $C_6H_{12}O_6 \cdot H_2O$, 44 g, Antifoam Struktol J650, 0.2 mL; PTM1, 4.35 mL; NH_4OH as N-source (concentration was determined by titration with 0.25 M potassium hydrogen phthalate).

Trace element solution (PTM1), per litre: $CuSO_4 \cdot 5H_2O$, 6.0 g; NaI 0.08 g; $MnSO_4 \cdot H_2O$, 3.0 g; $Na_2MoO_4 \cdot 2H_2O$, 0.2 g; H_3BO_3, 0.02 g; $CoCl_2$, 0.5 g; $ZnCl_2$, 20.0 g; $FeSO_4 \cdot 7H_2O$, 65.0 g; biotin, 0.2 g, H_2SO_4, 5 mL.

Feed glucose, per liter: glucose, 500 g; PTM1, 7.75 mL, Struktol J650, 0.3 mL.

Feed methanol, per liter: 300 g; PTM1, 7.75 mL, Struktol J650, 0.3 mL.

Adaption pulse, per liter: 0.5 % methanol.

Induction supplements, per liter: δ-Aminolevulinic acid (δ-Ala), 1 mM; $FeSO_4$, 1 mM.

9.4 Sequencing data

9.4.1 *E. coli* clones used for transformation into *P. pastoris* (reverse sequences not shown)

HRP_N57D_fwd sequenced

TTAATGCTTAGCGCAGTCTCTCTATCGCTTCTGAACCCCGGTGCACCTGTGCCGAA

ACGCAAATGGGGAAACACCCGCTTTTTGGATGATTATGCATTGTCTCCACATTGT

ATGCTTCCAAGATTCTGGTGGGAATACTGCTGATAGCCTAACGTTCATGATCAAA

ATTTAACTGTTCTAACCCCTACTTGACAGCAATATATAAACAGAAGGAAGCTGCC

CTGTCTTAAACCTTTTTTTTTATCATCATTATTAGCTTACTTTCATAATTGCGACTG

GTTCCAATTGACAAGCTTTTGATTTTAACGACTTTTAACGACAACTTGAGAAGATC

AAAAAACAACTAATTATTGAAAGAATTCAACGATGAGATTCCCATCTATTTTCAC

CGCTGTCTTGTTCGCTGCCTCCTCTGCATTGGCTGCCCCTGTTAACACTACCACTG

AAGACGAGACTGCTCAAATTCCAGCTGAAGCAGTTATCGGTTACTCTGACCTTGA

GGGTGATTTCGACGTCGCTGTTTTGCCTTTCTCTAACTCCACTAACAACGGTTTGT

TGTTCATTAACACCACTATCGCTTCCATTGCTGCTAAGGAAGAGGGTGTCTCTCTC

GAGAAGAGAGAGGCCGAAGCTCAACTTACTCCAACCTTCTACGATAACTCTTGTC

CTAATGTGTCCAACATCGTTAGAGACACCATTGTCAATGAATTGAGATCAGAT

CCACGTATTGCTGCATCTATCTTGAGACTTCACTTTCATGACTGCTTCGTCAACGG

TTGTGATGCTTCCATCTTGCTGGAC**GAC**ACTACCTCTTTCAGAACTGAGAAGGAC

GCTTTCGGTAATGCCAACTCTGCTAGAGGATTTCCAGTCATTGACAGAATGAAGG

CTGCCGTTGAATCTGCATGTCCTAGAACTGTGTCATGTGCTGACCTTCTGACTATT

GCCGCTCAGCAATCTGTTACCTTAGCTGGTGGACCATCCTGGAGAGTTCCATTGG

GTCGTAGAGACTCCCTTCAAGCCTTTCTGGACCTTGCAAATGCTAACTTGCCTGCT

CCATTCTTTACCTTACCTCAATTGAAAGACTCTTTCAGAAACGTTG

HRP_N57Q_fwd sequenced

AATCTCATTAATGCTTAGCGCAGTCTCTCTATCGCTTCTGAACCCCGGTGCACCTG

TGCCGAAACGCAAATGGGGAAACACCCGCTTTTTGGATGATTATGCATTGTCTCC

ACATTGTATGCTTCCAAGATTCTGGTGGGAATACTGCTGATAGCCTAACGTTCAT

GATCAAAATTTAACTGTTCTAACCCCTACTTGACAGCAATATATAAACAGAAGGA

AGCTGCCCTGTCTTAAACCTTTTTTTTTATCATCATTATTAGCTTACTTTCATAATT

GCGACTGGTTCCAATTGACAAGCTTTTGATTTTAACGACTTTTAACGACAACTTGA

GAAGATCAAAAAACAACTAATTATTGAAAGAATTCAACGATGAGATTCCCATCTA

TTTTCACCGCTGTCTTGTTCGCTGCCTCCTCTGCATTGGCTGCCCCTGTTAACACTA

CCACTGAAGACGAGACTGCTCAAATTCCAGCTGAAGCAGTTATCGGTTACTCTGA

CCTTGAGGGTGATTTCGACGTCGCTGTTTTGCCTTTCTCTAACTCCACTAACAACG

GTTTGTTGTTCATTAACACCACTATCGCTTCCATTGCTGCTAAGGAAGAGGGTGTC

TCTCTCGAGAAGAGAGAGGCCGAAGCTCAACTTACTCCAACCTTCTACGATAACT

CTTGTCCTAATGTGTCCAACATCGTTAGAGACACCATTGTCAATGAATTGAGATC

AGATCCACGTATTGCTGCATCTATCTTGAGACTTCACTTTCATGACTGCTTCGTCA

ACGGTTGTGATGCTTCCATCTTGCTGGAC**CAG**ACTACCTCTTTCAGAACTGAGAA

GGACGC

TTTCGGTAATGCCAACTCTGCTAGAGGATTTCCAGTCATTGACAGAATGAAGGCT

GCCGTTGAATCTGCATGTCCTAGAACTGTGTCATGTGCTGACCTTCTGACTATTGC

CGCTCAGCAATCTGTTACCTTAGCTGGTGGACCATCCTGGAGAGTTCCATTGGGT

CGTAGAGACTCCCTTCAAGCCTTTCTGGACCTTGCAAATGCTAACTTGCCTGCTCC

ATTCTTTACCTTACCTCAATTGAA

HRP_N57S_fwd sequenced

TTAATGCTTAGCGCAGTCTCTCTATCGCTTCTGAACCCCGGTGCACCTGTGCCGAA

ACGCAAATGGGGAAACACCCGCTTTTTGGATGATTATGCATTGTCTCCACATTGT

ATGCTTCCAAGATTCTGGTGGGAATACTGCTGATAGCCTAACGTTCATGATCAAA

ATTTAACTGTTCTAACCCCTACTTGACAGCAATATATAAACAGAAGGAAGCTGCC

CTGTCTTAAACCTTTTTTTTTATCATCATTATTAGCTTACTTTCATAATTGCGACTG

GTTCCAATTGACAAGCTTTTGATTTTAACGACTTTTAACGACAACTTGAGAAGATC

AAAAAACAACTAATTATTGAAAGAATTCAACGATGAGATTCCCATCTATTTTCAC

CGCTGTCTTGTTCGCTGCCTCCTCTGCATTGGCTGCCCCTGTTAACACTACCACTG

AAGACGAGACTGCTCAAATTCCAGCTGAAGCAGTTATCGGTTACTCTGACCTTGA

GGGTGATTTCGACGTCGCTGTTTTGCCTTTCTCTAACTCCACTAACAACGGTTTGT

TGTTCATTAACACCACTATCGCTTCCATTGCTGCTAAGGAAGAGGGTGTCTCTCTC

GAGAAGAGAGAGGCCGAAGCTCAACTTACTCCAACCTTCTACGATAACTCTTGTC

CTAATGTGTCCAACATCGTTAGAGACACCATTGTCAATGAATTGAGATCAGAT

CCACGTATTGCTGCATCTATCTTGAGACTTCACTTTCATGACTGCTTCGTCAACGG

TTGTGATGCTTCCATCTTGCTGGAC**AGC**ACTACCTCTTTCAGAACTGAGAAGGAC

GCTTTCGGTAATGCCAACTCTGCTAGAGGATTTCCAGTCATTGACAGAATGAAGG

CTGCCGTTGAATCTGCATGTCCTAGAACTGTGTCATGTGCTGACCTTCTGACTATT

GCCGCTCAGCAATCTGTTACCTTAGCTGGTGGACCATCCTGGAGAGTTCCATTGG

GTCGTAGAGACTCCCTTCAAGCCTTTCTGGACCTTGCAAATGCTAACTTGCCTGCT

CCATTCTTTACCTTACCTCAATTGAAAGACTCTTTCAGAAACGTTGGTCTTAACAG

ATCAT

9.4.2 Colony PCR

HRP_N57D_colony PCR sequenced

CAAAAAACAACTAATTATTGAAAGAATTCAACGATGAGNTTCCCATCTATTTTCA

CCGCTGTCTTGTTCGCTGCCTCCTCTGCATTGGCTGCCCCTGTTAACACTACCACT

GAAGACGAGACTGCTCAAATTCCAGCTGAAGCAGTTATCGGTTACTCTGACCTTG

AGGGTGATTTCGACGTCGCTGTTTTGCCTTTCTCTAACTCCACTAACAACGGTTTG

TTGTTCATTAACACCACTATCGCTTCCATTGCTGCTAAGGAAGAGGGTGTCTCTCT

CGAGAAGAGAGAGGCCGAAGCTCAACTTACTCCAACCTTCTACGATAACTCTTGT

CCTAATGTGTCCAACATCGTTAGAGACACCATTGTCAATGAATTGAGATCAGATC

CACGTATTGCTGCATCTATCTTGAGACTTCACTTTCATGACTGCTTCGTCAACGGT

TGTGATGCTTCCATCTTGCTGGAC**GAC**ACTACCTCTTTCAGAACTGAGAAGGAC

GCTTTCGGTAATGCCAACTCTGCTAGAGGATTTCCAGTCATTGACAGAATGAAGG

CTGCCGTTGAATCTGCATGTCCTAGAACTGTGTCATGTGCTGACCTTCTGACTATT

GCCGCTCAGCAATCTGTTACCTTAGCTGGNGGACCATCCTGGAGAGTTCCATTGG

GTCGNANAGACTCCCTTCAAGCCTTTCTGGACCTTGCAAATGCTAACTTGCCTGCT

CCATTCTTTACCTTACCTCAAT

HRP_N57Q_colony PCR sequenced

GATCAAAAAACAACTAATTATTGAAAGAATTCAACGATGANNTTCCCATCTATTT

TCACCGCTGTCTTGTTCGCTGCCTCCTCTGCATTGGCTGCCCCTGTTAACACTACC

ACTGAAGACGAGACTGCTCAAATTCCAGCTGAAGCAGTTATCGGTTACTCTGACC

TTGAGGGTGATTTCGACGTCGCTGTTTTGCCTTTCTCTAACTCCACTAACAACGGT

TTGTTGTTCATTAACACCACTATCGCTTCCATTGCTGCTAAGGAAGAGGGTGTCTC

TCTCGAGAAGAGAGAGGCCGAAGCTCAACTTACTCCAACCTTCTACGATAACTCT

TGTCCTAATGTGTCCAACATCGTTAGAGACACCATTGTCAATGAATTGAGATCAN

ANCCACGTATTGCTGCATCTATCTTGAGACTTCACTTTCATGACTGCTTCGTCAAC

GGTTGTGATGCTTCCATCTTGCTGGAC**CAG**ACTACCTCTTTCANAACTGANAAGG

HRP_N57S_colony PCR sequenced

GANGATCAAAAAACAACTAATTATTGAAAGAATTCAACGATGAGNTTCCCATCTA

TTTTCACCGCTGTCTTGTTCGCTGCCTCCTCTGCATTGGCTGCCCCTGTTAACACTA

CCACTGAAGACGAGACTGCTCAAATTCCAGCTGAAGCAGTTATCGGTTACTCTGA

CCTTGAGGGTGATTTCGACGTCGCTGTTTTGCCTTTCTCTAACTCCACTAACAACG

GTTTGTTGTTCATTAACACCACTATCGCTTCCATTGCTGCTAAGGAAGAGGGTGTC

TCTCTCGAGAAGAGAGAGGCCGAAGCTCAACTTACTCCAACCTTCTACGATAACT

CTTGTCCTAATGTGTCCAACATCGTTAGAGACACCATTGTCAATGAATTGAGATC

AGATCCACGTATTGCTGCATCTATCTTGAGACTTCACTTTCATGACTGCTTCGTCA

ACGGTTGTGATGCTTCCATCTTGCTGGAC**AGC**ACTACCTCTTTCAGAACTGAGAA

GGACGCTTTCGGTAATGCCAACTCTGCTAGAGGATTTCCAGTCATTGACAGAATG

AAGGCTGCCGTTGAATCTGCATGTCCTAGAACTGTGTCATGTGCTGACCTTCTGAC

TATTGCCGCTCAGCAATCTGTTACCTTAGCTGGTGGACCATCCTGGAGAGTTCCAT

TGGGTCGTANAGACTCCCTTCAAGCCTTTCTGGACCTTGCAAATGCTAACTTG

CCTGCTCCATTCTTTACCTTACCTCAATTGAAAGACTCTTTCAGAAACGTTGG